

Zinc Complexes of Piperazinyl-aminephenolate Ligands: Synthesis, Characterization and Ring-Opening Polymerization Activity

Nduka Ikpo,^[a] Lisa N. Saunders,^[a] Jillian L. Walsh,^[a] Jennifer M. B. Smith,^[a] Louise N. Dawe,^[b] and Francesca M. Kerton *^[a]

Keywords: Zinc / Alkyl / Alkoxide / Phenoxide / Ring-opening polymerization / Lactide / Caprolactone / Carbon dioxide

A series of zinc complexes was prepared from 2(*N*-piperazinyl-*N'*-methyl)-2-methylene-4-R'-6-R-phenols ($[\text{ONN}^{\text{R}',\text{R}}]\text{JH}$) [$\text{R}' = \text{Me}$, $\text{R} = {'}\text{Bu}$, (**L1H**); $\text{R}' = \text{R} = {'}\text{Bu}$, (**L2H**); $\text{R}' = \text{R} = {'}\text{Am}$, {*tert*-Amyl} (**L3H**)] and characterized through elemental analysis, ^1H and $^{13}\text{C}\{^1\text{H}\}$ NMR spectroscopy, and X-ray crystallography. Reaction of ZnEt_2 with **L1H-L3H** gave $\text{Zn}[\text{ONN}^{{'}\text{Bu},{'}\text{Bu}}]_2$ (**1**) as a monometallic complex and $\{[\mu\text{-ONN}^{\text{R}',\text{R}}]\text{ZnEt}\}_2$ (**2-4**) as bimetallic species with distorted tetrahedral environments about the Zn centres. Reaction of **3** and **4** with alcohols gave $\{[\text{ONN}^{\text{Am},{'}\text{Am}}]\text{Zn}(\mu\text{-OR''})\}_2$ (**5**) and (**6**)

bimetallic species with Zn centres bridged by benzyl alkoxide and ethoxide groups, respectively. A morpholinyl derived ligand was also synthesized and characterized (**L4H**) and its 1:1 stoichiometric reaction with ZnEt_2 resulted in complex **7**, $\{[\mu\text{-ONO}^{{'}\text{Bu},{'}\text{Bu}}]\text{ZnEt}\}_2$. The reactivity of complexes **2-7** in the ring opening polymerization of *rac*-lactide and ϵ -caprolactone was studied. Reactions of carbon dioxide with cyclohexene oxide in the presence of **6** or **7/ROH** afforded cyclohexene carbonate.

Introduction

Amine-phenolate and related ligands possessing a mixed set of N- and O- donor atoms have attracted a great deal of interest over the past decade due to their ability to coordinate to a range of metal centres and the ease of systematic steric control by variation of the backbone and phenol substituents.^[1-23] Various ligands of this type have been used in main group and early transition metal chemistry (including lithium,^[2-3] magnesium,^[4-10] calcium,^[11] rare earths,^[12, 13] zinc,^[1, 14-17, 19] aluminum,^[18, 20] zirconium^[21, 22] and titanium.^[23]) Many of these complexes have been reported to be excellent initiators for ring-opening polymerization (ROP) of cyclic esters such as *rac*-lactide. The quest is ongoing for new systems that can advance our understanding of this reaction and ultimately lead to a better-controlled performance in this and other polymerization reactions.

Recently, Issenhuth *et al.* reported the synthesis of cationic aluminum complexes supported by morpholinyl-aminephenolate ligands as efficient initiators for ROP of propylene oxide.^[24] Of particular relevance to the current study, Carpenter and co-workers recently described the synthesis of zinc and magnesium complexes supported by ether-aminephenolate ligands, including those bearing morpholinyl side-arms, as effective initiators for immortal ROP of cyclic esters.^[25] Also, Lappert and co-workers have reported zinc complexes stabilized by a piperazinylphenolate ligand,^[26] one such complex was found to uptake some CO_2 when attempts at cyclohexene oxide- CO_2 copolymerizations were undertaken although no polymer was isolated.

In this paper, we describe the synthesis and structural characterization of a group of piperazinyl phenol ligands and a morpholinyl phenol ligand, their coordination chemistry with Zn and their use as single and/or binary-component initiators for the ring-opening polymerization (ROP) of *rac*-lactide and ϵ -caprolactone under various conditions, including under microwave (MW) irradiation. MW irradiation has not been used extensively in ROP of lactide facilitated by metal complexes.^[27, 28] In the two examples reported to date simple tin initiators, e.g. stannous octoate, were used and the resulting polymers have broad polydispersities. High reaction temperatures are normally detrimental to achieving controlled polymerization, however, MWs allow rapid heating of reaction mixtures. Sluggish initiators, e.g. those bearing ligands with sterically demanding groups, normally require heating to obtain a worthwhile reaction rate. In such cases, MW heating may lead to a reduction in the number of side-reactions, e.g. transesterification, by reducing the overall reaction time. Also, MW heating could lead to more rapid screening of potential ROP initiators.

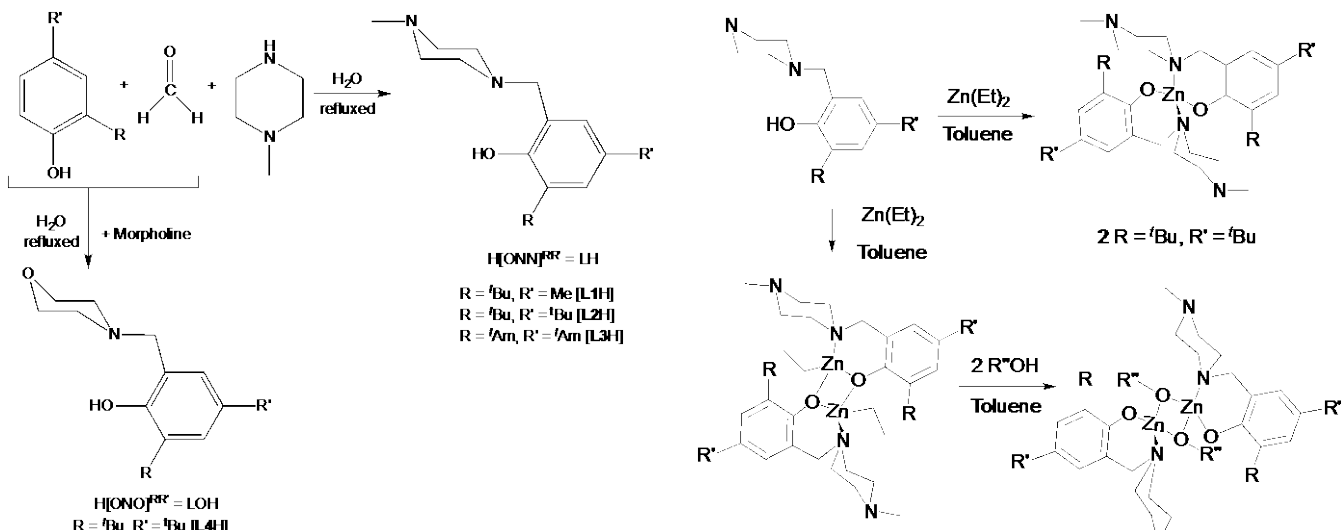
In this article, we also describe our initial studies towards the reactivity of these complexes with carbon dioxide, as many Zn phenolate and alkoxide complexes have shown good activity towards either copolymerization of CO_2 with epoxides or the formation of cyclic carbonates,^[29, 30]

Results and Discussion

The protio ligands were synthesized from the appropriate phenol, formaldehyde and 1-methylpiperazine *via* a modified Mannich condensation reaction, as shown in Scheme 1. They were isolated in excellent yields. **L2H** has been previously prepared through a slightly different procedure that involved reduction with hydrobromic acid and neutralization with aqueous NaHCO_3 ,^[26] however, its molecular structural data have not been reported. The preparation of **L4H** has been reported previously through a Mannich condensation reaction in 1,4-dioxane under reflux.^[25]

[a] Department of Chemistry, Memorial University of Newfoundland, St. John's, NL, A1B 3X7, Canada
Fax: +17098643702
E-mail: fkerton@mun.ca
[b] X-ray Crystallography Laboratory, Centre for Chemical Analysis, Research and Training, Memorial University of Newfoundland, St. John's, NL, A1B 3X7, Canada

 Supporting information for this article is available on the WWW under <http://www.eurjic.org/> or from the author.



Scheme 1. Synthesis of amine-phenolate ligand precursors

The recently reported benign route (reaction in water)^[31]^[31, 32] to amine-phenol ligands proved to reduce the amount of reagents used and afforded high yields of **L1H-L4H**. These were recrystallized from methanol by cooling to 0 °C. Their characterization by ¹H- and ¹³C{¹H} NMR studies afforded well resolved resonances for all proton and carbon environments, while elemental analysis showed that the compounds were obtained in pure form. Single crystals of **L2H** suitable for X-ray crystallography were grown *via* slow evaporation of a saturated methanol solution at ambient temperature. The solid-state structure of **L2H** shown in Fig.1 reveals intramolecular hydrogen bonding between the phenol and the proximal amine. The *N*-methylpiperazine ring adopts the normal chair conformation. Tables 5 and 6 summarize crystal data for all structures reported in this article.

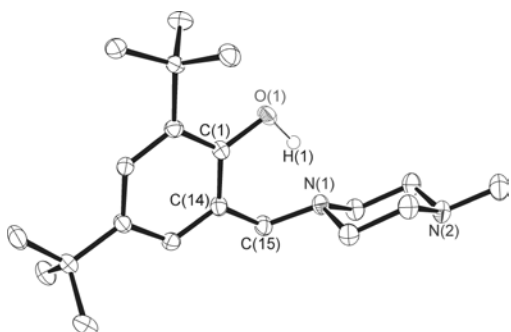
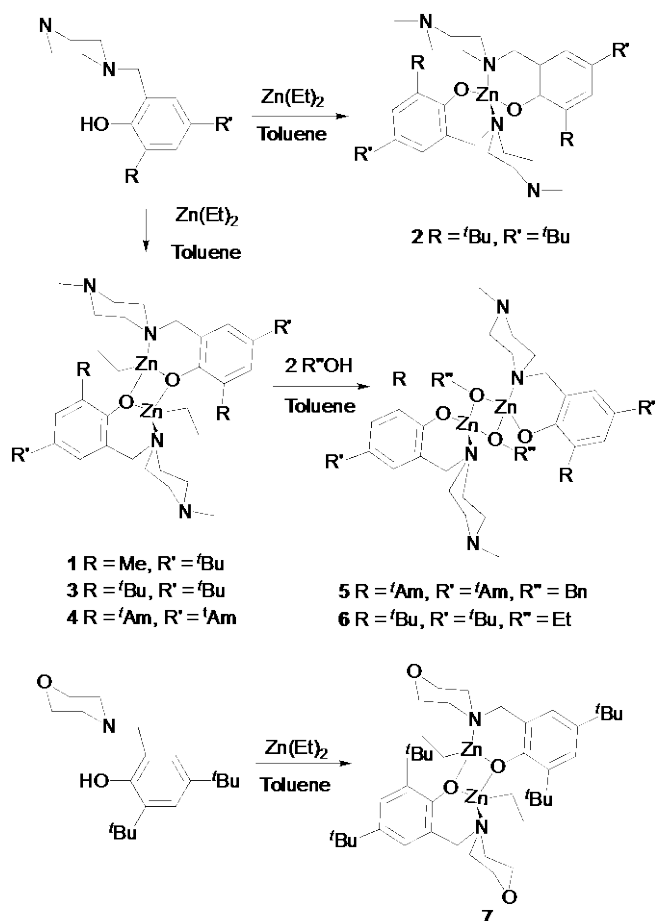


Figure 1. Molecular structure of **L2H**. (50% thermal ellipsoids; H1 atom included). Selected bond lengths (Å) and bond angles (°): O(1)-C(1), 1.366(2); N(1)-C(15), 1.472(2); C(14)-C(15), 1.516(2); O(1)-C(1)-C(14), 119.73(14); O(1)-C(1)-C(2), 119.76(14); N(1)-C(15)-C(14), 113.72(14)

Synthesis and characterization of zinc aminephenolate complexes

Reactions of protio ligands [ONN^{R,R'}]H with ZnEt₂ in toluene under ambient conditions led to the isolation of molecular zinc complexes Zn[ONN^{tBu,tBu}]₂ (**1**) and {[μ-ONN^{R,R'}]ZnEt₂}₂ (**2-4**) in 56-96% yield (Scheme 2). Treatment of complexes **3** and **4** with two equivalents of benzyl alcohol and ethanol respectively in toluene at ambient temperature afforded **5** and **6**. An equimolar reaction between **L4H** and ZnEt₂ afforded {[μ-ONO^{tBu,tBu}]ZnEt₂}₂ (**7**) in 81% yield.



Scheme 2. Synthetic procedure of amine-phenolate zinc complexes

The synthesis of a monometallic zinc complex related to **1** has been reported by Lappert and co-workers *via* the indirect route of reacting a bimetallic phenolate-bridged ethyl zinc complex with 2 equiv. of methanol.^[26] Another similar monometallic zinc complex was reported by Sobota and co-workers from the reaction of 2 equiv. of an amine-phenol ligand with 1 equiv. of ZnEt₂.^[33] In our case both the monometallic (**1**) and bimetallic (**2** and **4**) zinc complexes were synthesized by reaction of 1:1 equiv. of ZnEt₂ with the corresponding ligands. Although all reactions were carried out under rigorous air- and moisture-free conditions, we cannot rule out the potential role of adventitious water for the isolation of **1** under such conditions. In this regard, the isolation of **1** would be similar to the route reported by Lappert using methanol as a proton source. Nevertheless, the reaction of **L2H** with an excess of ZnEt₂ in toluene did lead to the formation of the desired bimetallic zinc complex (**2**). Treatment of complexes **3** and **4** with 2 equiv. of ethanol and benzyl alcohol respectively afforded alkoxy-bridged complexes (**5**) and (**6**).

The zinc complexes **1-7** were characterized by elemental analyses, ¹H and ¹³C{¹H} NMR spectroscopy. The ¹H NMR spectra of **1-7** in C₅D₅N solvent at room temperature showed broad resonances in the methylene (PhCH₂N) and amine methyl regions, which prompted variable temperature NMR studies of the complexes. A portion of a representative variable temperature spectrum, of **4**, is shown in Figure 2. At elevated temperature (343 K), sharp signals were discerned which were very informative for establishing the formation of the complexes **1-7**. Complex **1** exhibits three sharp singlets for the aromatic and methylene protons at 7.58, 7.11 and 4.07 ppm, which have shifted from 7.26, 6.93 and 3.75 ppm in the free ligand (**L2H**), and no Zn-ethyl resonances were observed. In contrast, the methylene (PhCH₂N) protons for **3** shifted to 3.65 ppm and additional signals were observed at 0.59 and 1.57 ppm as a quartet and a triplet

corresponding to the ethyl group on the zinc ion. Similar resonances are observed for complexes **2**, **4** and **7**. Upon lowering the temperature, the methylene signals became broader for all the complexes, which implied that at high temperature there is fast exchange of a coordinated pyridine or the coordinated piperazine ligand and free pyridine solvent on the NMR time scale. It should also be noted that in solution the bimetallic species (analogous to their solid-state structures) are unlikely to exist in the presence of such a large quantity of Lewis base (C_5D_5N). However, use of this solvent was essential in gaining sufficient solubility for all samples studied and to allow direct comparison of their spectra.

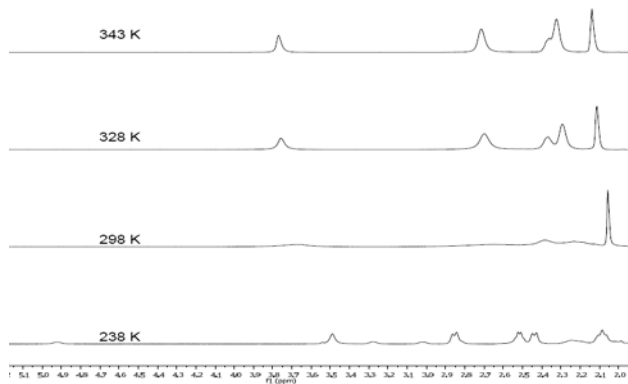


Figure 2. Variable temperature ^1H NMR spectra of the methylene region of **4** in C_5D_5N .

X-ray crystallographic analyses of zinc complexes

Crystal structures of complexes **1-7** were determined by X-ray diffraction analysis. The molecular structure of complex **1** is shown in Figure 3 along with selected bond lengths and angles. The central zinc atom adopts a distorted tetrahedral geometry coordinated by four donor atoms from two piperazinyl aminephenolate ligands. The fact that one of the amine nitrogen atoms remains pendant can be attributed to the restriction of the chair conformation adopted by the piperazinyl unit of the ligand, which orients N(2) away from the central metal atom. Future studies will involve investigating chemistry at this nitrogen centre. The structure of **1** is centrosymmetric (the zinc ion is located on a crystallographic inversion centre) with Zn-O and Zn-N distances within the normal ranges for related complexes. The more acute bond angles around Zn, O(1)-Zn(1)-N(1) 96.82(5) $^\circ$, can most probably be associated with the bite of the six-membered $C_3N\text{Zn}O$ chelate ring. This ring adopts a legless chair^[34] or slight sofa^[11] conformation with the C(6) atom forming the backrest and lies *ca.* 0.76 Å out of Zn(1)-O(1)-C(20)-C(7)-N(1) plane.

The ORTEP drawing of **2** is presented in Figure 4 along with selected bond lengths and angles. The structure exhibits a butterfly-like arrangement with the two ethyl groups positioned on the same side with respect to the Zn_2O_2 core plane, while the two piperazine units are situated on the opposing side of the Zn_2O_2 plane. This *cisoid* conformation of ethyl groups is rare in zinc ethyl chemistry, although an example has been reported.^[35] Each zinc ion adopts a distorted tetrahedral geometry consisting of two bridging phenolate oxygen atoms, one nitrogen donor and one ethyl group. The central metal ring Zn_2O_2 displays a twisted geometry with O(1) and O(2) *ca.* 0.54 and 0.55 Å off the plane of O(2)-Zn(1)-Zn(2) and O(1)-Zn(1)-Zn(2) respectively. The angles at the central atoms Zn(1) [80.47(8) $^\circ$] and Zn(2) [80.89(8) $^\circ$] are narrower than the corresponding bridging oxygen angles O(1) [97.75(9) $^\circ$] and O(2) [96.55(9) $^\circ$]. The acute angles are likely a result of the six-membered chelate ring enforced by the ligand. The two C_3OZnO chelate rings adopt boat conformations with C(6) and O(1) *ca.* 0.62

and 0.71 Å off the plane of Zn(1)-C(17)-C(7)-N(1), while C(23) and O(2) are *ca.* 0.64 and 0.74 Å off the plane of Zn(2)-C(34)-C(24)-N(2). The Zn-C bond distances in **2** are comparable to those in related complexes and from a survey of the literature,^[36] where mean Zn-C bond distances in such species are 1.978 Å. Of those complexes that are bimetallic, the ethyl groups are transoidal.^[21,37,38] The Zn-O bond distances are similar to the mean distance [2.039 Å] from a literature survey and are comparable with related zinc complexes reported in the literature.^[26,35,38-41] The Zn(1)-Zn(2) distance [3.0527(6) Å] is close to that reported by Gibson [3.0276(5) Å], while the O(1)-O(2) separation distance [2.634 Å] is shorter [2.817 (3) Å].^[11]

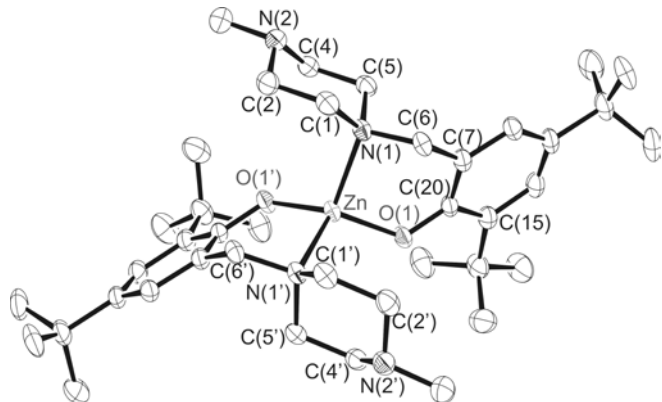


Figure 3. Molecular structure of **1**. (50% thermal ellipsoids; H atoms excluded for clarity). The two halves of the molecule are symmetry related by an inversion centre. Selected bond lengths (Å) and bond angles ($^\circ$): Zn(1)-O(1), 1.9008(11); Zn(1)-N(1), 2.1198(13); O(1)-C(20), 1.3357(17); N(1)-C(1), 1.4885(19); N(1)-C(5), 1.4909(19); N(1)-C(6), 1.4982(19); N(2)-C(2), 1.453(2); N(2)-C(3), 1.454(2); N(2)-C(4), 1.463(2); C(1)-C(2), 1.520(2); C(4)-C(5), 1.510(2); C(15)-C(20), 1.422(2); O(1)-Zn(1)-O(1), 124.94(7); O(1)-Zn(1)-N(1), 110.52(5); O(1)-Zn(1)-N(1'), 96.82(5); C(20)-O(1)-Zn(1), 125.45(10); C(1)-N(1)-C(6), 108.82(12); C(1)-N(1)-Zn(1), 114.91(9); C(6)-N(1)-Zn(1), 102.40(9); N(1)-C(1)-C(2), 111.18(13).

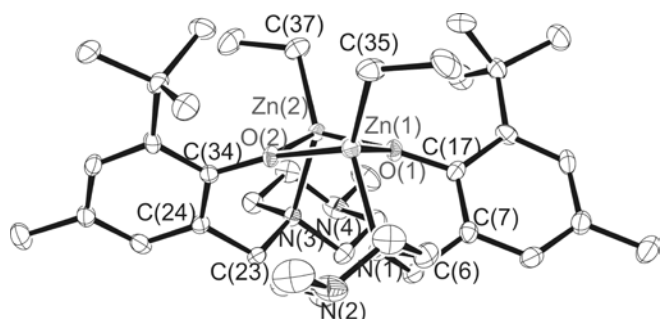


Figure 4. Molecular structure of **2**. (50% thermal ellipsoids; H atoms excluded for clarity). Selected bond lengths (Å) and bond angles ($^\circ$): Zn(1)-C(35), 1.981(3); Zn(1)-O(1), 2.037(2); Zn(1)-O(2), 2.043(2); Zn(1)-N(1), 2.148(3); Zn(1)-Zn(2), 3.0527(6); Zn(2)-C(37), 1.991(3); Zn(2)-O(1), 2.015(2); Zn(2)-O(2), 2.047(2); Zn(2)-N(3), 2.143(3); O(1)-C(17), 1.361(3); O(2)-C(34), 1.353(3); C(35)-Zn(1)-O(1), 117.75(13); C(35)-Zn(1)-O(2), 124.72(12); C(35)-Zn(1)-N(1), 123.31(12); O(1)-Zn(1)-N(1), 93.77(9); O(2)-Zn(1)-N(1), 105.03(9); C(37)-Zn(2)-O(1), 123.41(12); C(37)-Zn(2)-O(2), 115.93(12); O(1)-Zn(2)-O(2), 80.89(8); Zn(2)-O(1)-Zn(1), 97.75(9); Zn(1)-O(2)-Zn(2), 96.55(9).

The single crystal structure determination of complex **3** depicted in Figure 5 reveals a centrosymmetric bimetallic complex with the zinc centres bridged through the oxygen atoms of the phenolate ligands. The geometry at the zinc atom is distorted tetrahedral. It should be noted that the bond angle of O(1)-Zn(1)-O(1') [83.78(13) $^\circ$] is wider than that in Bochmann's $[\text{EtZn}(\mu-\text{OC}_6\text{F}_5)(\text{py})_2]$ complex [78.00(5) $^\circ$], which contains a *trans*-alkyl

zinc centre with a phenolate ligand and a nitrogen donor (in that case, pyridine).^[42] The similarities in the types of donors in the coordination sphere of Zn in each complex allows the difference in the bond angles to be attributed to the chelate bite-angle of **L2** in complex **3**, whereas the donors in Bochmann's complex are not linked and free to orientate themselves with minimal constraint. In **3**, C(15) and O(1) lie *ca.* 0.75 and 0.45 Å off the mean plane of Zn(1)-N(1)-C(6)-C(1), inducing a chair conformation chelate ring, while the zinc atoms lie *ca.* 0.58 Å above the plane of the coordinated N(1), C(21) and O(1) atoms. The central Zn₂O₂ ring is planar with the angle at Zn(1) narrower than that at O(1). The Zn-C, Zn-N and Zn-O bond distances are within the ranges previously reported for zinc complexes.^[1,26,39,43] The ethyl groups on each of the two metal centres lay *trans* to each other. Presumably, the larger *tert*-butyl group in the 4-position of the phenolate donor in **3**, although distant from the metal coordination sphere, causes the ethyl groups to orientate themselves in a *trans* arrangement in contrast to the *syn*-(*cis*) arrangement in **2**, where the 4-position of the phenolate group is a methyl.

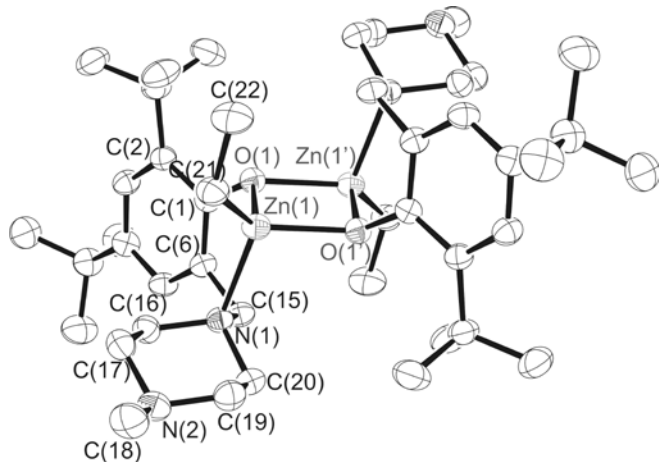


Figure 5. Molecular structure of **3**. (50% thermal ellipsoids; H atoms excluded for clarity). The two halves of the molecule are symmetry related by an inversion centre. Selected bond lengths (Å) and bond angles (°): Zn(1)-C(21), 1.977(4); Zn(1)-O(1), 2.052(3); Zn(1)-N(1), 2.185(4); Zn(1)-Zn(1), 3.068(5); O(1)-C(1), 1.362(3); N(1)-C(20), 1.479(4); N(1)-C(16), 1.483(4); N(1)-C(15), 1.498(4); N(2)-C(17), 1.457(4); N(2)-C(18), 1.458(4); N(2)-C(19), 1.460(4); C(1)-C(2), 1.416(4); C(21)-Zn(1)-O(1), 124.87(11); O(1)-Zn(1)-O(1'), 83.78(13); C(21)-Zn(1)-N(1), 118.53(16); O(1)-Zn(1)-N(1), 92.53(10); O(1)-Zn(1)-N(1'), 103.06(11); C(1)-O(1)-Zn(1), 117.95(18); C(1)-O(1)-Zn(1'), 123.86(17); Zn(1)-O(1)-Zn(1'), 96.22(13); C(20)-N(1)-C(16), 106.4(2); C(20)-N(10)-C(15), 107.5(2); C(16)-N(1)-C(15), 110.1(2); C(20)-N(1)-Zn(1), 113.99(18); C(16)-N(1)-Zn(1), 114.17(18).

The single crystal X-ray data for **4** were poor due to merohedral twinning and weak diffraction however the structure and connectivity was confirmed and authenticates its structural analogy to **3**. A ball and stick model of **4** is available in Supporting Information.

Reaction of the alkyl complexes with alcohols afforded alkoxy-bridged complexes. Suitable single crystals were grown through slow evaporation of a hexane/toluene mixture (**5**) and from a saturated toluene solution at -35 °C (**6**). The molecular structures reveal the bimetallic nature of these species. An ORTEP drawing of **6** is shown in Figure 6 and the structure of **5** is available in Supporting Information. The zinc centres adopt distorted tetrahedral geometries bridged by the oxygen atoms of the ethoxide or benzyl alkoxide groups to form a Zn₂O₂ planar core. Comparison between the angles of the Zn₂O₂ planar core for complexes **5** and **6** reveals that the O-Zn-O bond angle in **6** is slightly narrower than that in complex **5**, while the Zn-O-Zn bond angle is wider in complex **6** than in complex **5**. The bond lengths within the two complexes are similar and **6** contains bond distances comparable to a related ethoxide-bridged zinc species.^[44]

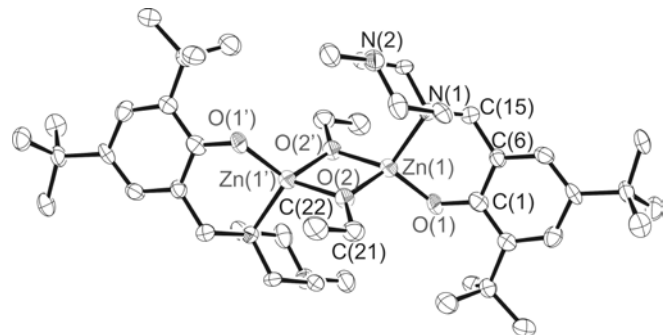


Figure 6 Molecular structure of **6**. (50% thermal ellipsoids; H atoms excluded for clarity). Selected bond lengths (Å) and bond angles (°): Zn(1)-N(1), 2.088(6); Zn(1)-Zn(1), 2.954(2); O(1)-C(1), 1.330(8); O(2)-C(21), 1.404(8); O(2)-Zn(1), 1.957(5); O(2)-Zn(1)-O(2), 82.0(2); O(1)-Zn(1)-N(1), 100.8(2); O(2)-Zn(1)-N(1), 117.4(2); C(21)-O(2)-Zn(1), 131.9(4); Zn(1)-O(2)-Zn(1'), 98.0(2).

Crystals of complex **7** were obtained by cooling a saturated toluene solution to -35 °C. The solid-state structure of complex **7** (Figure 7), like the related piperazinyl complex **3**, contains zinc atoms coordinated by the phenolate oxygen atom and the proximal nitrogen atom of the ligand to form a Zn₂O₂ planar core. The bond angles and distances are in the range of the known bimetallic zinc phenolate complexes and comparable with **3**.^[1,26,39,43]

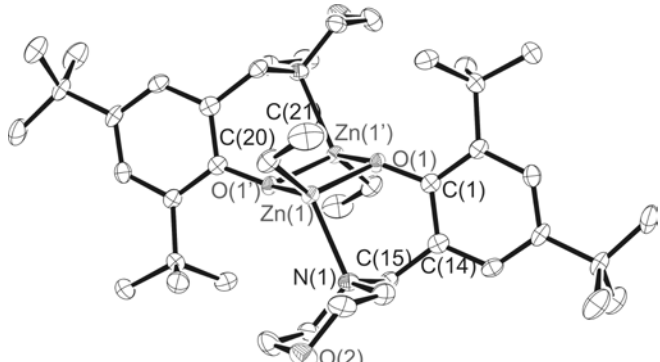


Figure 7. Molecular structure of **7**. (50% thermal ellipsoids; H atoms excluded for clarity). The two halves of the molecule are symmetry related by an inversion centre. Selected bond lengths (Å) and bond angles (°): Zn(1)-C(20), 1.956(6); Zn(1)-O(1), 2.071(4); Zn(1)-N(1), 2.177(5); Zn(1)-Zn(1), 3.0608(14); O(1)-C(1), 1.354(7); O(2)-C(17), 1.393(8); C(20)-Zn(1)-O(1), 128.8(2); C(20)-Zn(1)-O(1'), 115.6(2); O(1)-Zn(1)-O(1), 82.87(17); C(20)-Zn(1)-N(1), 121.1(2); O(1)-Zn(1)-N(1), 92.70(18); C(1)-O(1)-Zn(1), 119.1(3).

Polymerization of cyclic esters

Ring-opening polymerization of *rac*-lactide.

The activity of complexes **2-5** and **7** as initiators for ROP of *rac*-lactide was examined in toluene (Table 1 and Figure 8) and neat (Table 2). Compound **7** has been studied previously by Carpenter and co-workers.^[25] It is included here for comparative purposes and afforded a polymer with relatively narrow M_w/M_n . For the piperazinyl-derived initiators, M_w/M_n for PLA were between 1.25 and 1.87. Reaction rates generally correlated with both the steric demand of the ligand and co-initiator (alcohol) with **2** and BnOH affording near quantitative conversions within shorter times than its *'Am* and *'Bu* analogs and was comparable in its activity with compound **7**. Overall the molecular weights (M_n) of the polymer samples were lower than the expected values based on % conversion. This deviation likely implies that some transesterification reactions and/or a slow initiation step relative to propagation occurred. Both the broadening of molecular weight distribution and deviation from expected M_n increased with

$[LA]_0:[Zn]_0$ ratio (entries 2 and 3, entries 6–8), and increased with reaction time and temperature. These trends are frequently observed in ROP of cyclic esters.^[45–47] In an attempt to distinguish between a less-controlled polymerization due to slow initiation versus transesterification, the single-component initiator **5** was studied (Table 1, entry 12). M_w/M_n for the resulting polymer was not significantly different to that obtained for PLA under similar conditions using **4/BnOH** (Table 1, Entry 11). However, as expected, **5** did result in more rapid polymerization than **4/BnOH**. The difference in the rate of polymerization could be attributed to a time lapse in transforming the precursor alkyl species upon alcoholysis into the active alkoxide complex.

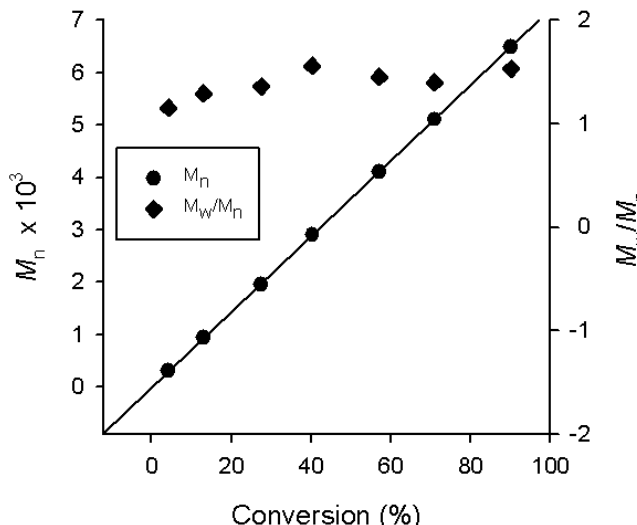


Figure 8. Plots of molecular weight M_n and PDI (M_w/M_n determined by GPC) vs monomer conversion for **3/BuOH**-initiated ROP of *rac*-lactide. Conditions: $[LA]:[Zn]:[BuOH] = 50:1:1$, $[Zn]_0 = 18.2$ mM, toluene, 60°C , 0.1 mL aliquots taken at the given intervals. Diamonds correspond to M_w/M_n and circles to M_n .

For the Zn-alkyl species, the presence of alcohol was necessary to generate an efficient initiator system for the polymerization of *rac*-lactide as has been reported in the literature.^[48–49] The use of BnOH and *t*BuOH as co-initiators with **3** was studied using conventional heating and MW irradiation. It was noted that conversions of 90% and 93% could be reached in 5 min for *t*BuOH and BnOH respectively (entries 9 and 10) using MW but similar conversions using conventional heating required significantly longer reaction times, particularly for *t*BuOH compared with BnOH (entries 4 and 5). The M_n of the PLA prepared using MW showed good agreement with the theoretical values. These data imply that MW can be used to assist control in ROP when bulky co-initiators are used, as there is a less apparent difference in initial reaction rate under such conditions compared with conventional heating. This could be particularly useful in the preparation of star-polymers and other systems where a sterically congested co-initiator is required. It should be noted that in the conventionally heated reactions, solutions of monomer and initiator were heated separately and then mixed once the desired reaction temperature was achieved.

Microstructural analyses of the resulting PLA were performed through inspection of the methine region of the homodecoupled ^1H NMR spectra. P_r values were generally close to 0.5 indicating that atactic polymer was produced. Reactions with good initiation rates (entries 4, 9, 10 and 12) afforded polymers with a very slight isotactic bias ($P_r = 0.45\text{--}0.47$) whereas longer reaction times and higher temperatures (excl. MW) gave polymers with a very slight heterotactic bias ($P_r = 0.51\text{--}0.55$). The latter polymers on average had broader molecular weight distributions than those with $P_r < 0.5$. Therefore, the apparent increase in heterotacticity is likely an artifact of transesterification reactions, and the small degree of isotacticity is probably induced through a chain-end control

mechanism. Occurrence of transesterification was confirmed via MALDI-TOF MS and ^1H NMR end-group analysis of the polymers. In mass spectra, two main series of signals were observed separated by a difference of 72 in m/z . These were assigned to open chain (even-mass) polymers and oligomers clustered with Na^+ and K^+ ions. Two less intense series of signals (80% less intense than the main series), separated by a m/z of 72, were also observed. These weaker signals were assigned to cyclic (odd-mass) polymers and oligomers clustered with Na^+ and K^+ ions. ^1H NMR spectra of the polymers in this paper all contained resonances attributable to OH end groups. However, integration of either the -OH or RO- end-group resonances relative to the methine protons generally afforded higher molecular weights than those obtained through either GPC or MALDI-TOF MS analysis, up to three times higher for polymers with the broadest M_w/M_n in our study. Therefore, ^1H NMR end-group analysis confirms that intramolecular transesterification had occurred, which produced cyclic species and led to less intense than predicted end-group resonances based on M_n data. Our results contrast with the previously reported work of Carpentier and co-workers where no transesterification was apparent (narrower molecular weight distributions and MALDI-TOF MS studies) and a heterotactic bias was observed in the resulting polymers ($P_r = 0.60$),^[25] although to achieve a heterotactic bias THF was used as the solvent, while in toluene a slight isotactic bias was observed ($P_r = 0.46$), in line with our piperazinyl systems. For the single morpholinyl-derived initiator in our study, we found $P_r = 0.49$ for the PLA formed in toluene, entry 13. The first-order plot for solution polymerization using this initiator (Fig. 9) was linear with k_{app} of 0.263 min^{-1} . Apparent rates observed for piperazinyl-derived species in this study were between 0.010 and 0.030 min^{-1} both in toluene and in molten *rac*-lactide. These data suggest that the morpholinyl-derived systems are superior initiators compared with their piperazinyl analogs in terms of fast reaction rate and greater degree of control. We propose that the outer sphere ether group may play a role in directing the incoming monomer for reaction at the metal centre and that the outer sphere tertiary amine group is less efficient in this process.

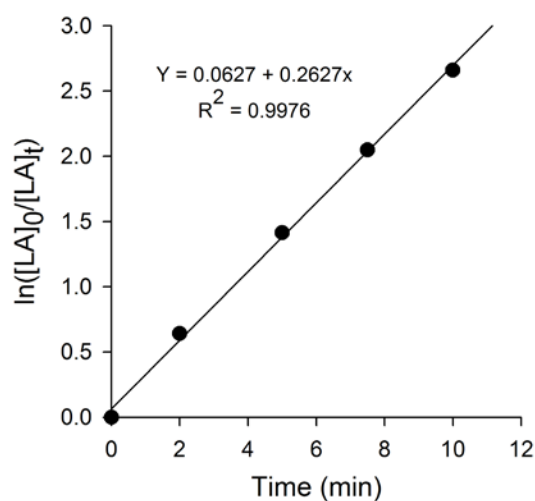


Figure 9. First-order plot of *rac*-lactide consumption using **7/BnOH** at 60°C . Conditions: $[LA]:[Zn]:[ROH] = 100:1:1$, 10 mL toluene, $[Zn]_0 = 32.0$ mM.

ROP reactions using the single-component initiators **5** and **6** were also performed under solventless conditions at 130°C , Table 2. Conversions reached more than 90% over 2 h (Table 2, entries 1 and 6) suggesting slow initiation compared with analogous solution phase polymerizations. The first-order plots for the bulk polymerization of *rac*-lactide using **5** and **6** as initiators (Fig. S7) were linear with k_{app} of 0.0179 and 0.0247 min^{-1} respectively. Bulk polymerization of *rac*-lactide in the presence of **6** (an ethoxide complex) is moderately faster than in the presence of **5** (a benzyl

alkoxide species) due to the differences in steric demand of the initiating alkoxide ligands. **5** afforded higher molecular weight polymers than **6**. M_n of these polymers were also significantly higher than the predicted values ($M_{n\text{cal}}$), which might be attributed to decomposition of the initiators at the high temperature required

for melt polymerization. Initiator decomposition leading to higher than expected M_n has been previously observed by Drouin *et al.*^[50] Both systems afforded predominantly atactic polymer under these reaction conditions due to the high temperature used.

Table 1. Ring-opening polymerization of *rac*-lactide initiated by complexes **2–5, 7** in toluene

Entry	Initiator	[LA] ₀ /[Zn] ₀ /[ROH] ₀	t/min	T/°C	Conv (%) ^d	$M_{n\text{cal}}^e \times 10^3$	$M_n^f \times 10^3$	M_w/M_n^f	P_r^g
1	2	100/1/1 ^a	60	60	97.1	13.9	10.9	1.25	0.49
2	2	100/1/1 ^a	10	60	96.0	13.8	7.99	1.23	0.49
3	2	200/1/1 ^a	15	60	96.3	27.7	11.8	1.39	0.53
4	3	100/1/1 ^a	90	70	98.0	14.1	13.6	1.32	0.45
5	3	100/1/1 ^b	120	70	96.4	13.9	12.0	1.60	0.53
6	3	100/1/0	120	70	0.1	-	-	-	-
7	3	200/1/1 ^b	120	70	98.0	28.2	13.3	1.76	0.55
8	3	300/1/1 ^b	120	70	98.3	42.5	15.3	1.87	0.49
9	3	100/1/1 ^b	5	120 ^c	90.0	12.9	12.0	1.33	0.47
10	3	100/1/1 ^a	5	120 ^c	93.6	13.5	9.19	1.42	0.47
11	4	100/1/1 ^a	60	70	97.0	11.4	12.3	1.42	0.51
12	5	100/1/0	15	70	94.9	13.7	10.0	1.37	0.47
13	7	100/1/1 ^a	30	60	97.6	13.9	9.56	1.25	0.49

^aIn presence of one equivalent of benzyl alcohol. ^bIn presence of one equivalent of *tert*-butyl alcohol. ^cMicrowave reaction (MW). ^dDetermined from ¹H NMR. ^e $M_{n\text{cal}}$ of polymer calculated from $M_{n\text{cal}} = ([\text{rac-LA}]_0/[\text{Zn}]_0) \times 144.13 \times \text{conversion (\%)} / 100$. ^fDetermined by GPC (chloroform), relative to polystyrene standards. The M_n was calculated according to $M_n = 0.58M_{n\text{GPC}}$. ^g P_r is the probability of racemic enchainment of monomers units, determined by homodecoupled ¹H NMR spectra according to Coates *et al.*^[51]

Table 2. Bulk polymerization of *rac*-lactide initiated by complexes **5** and **6** at 130 °C

Entry	Initiator	[LA] ₀ /[I] ₀	t /min	Conv. (%) ^a	$M_{n\text{cal}}^b \times 10^3$	$M_n^c \times 10^3$	M_w/M_n^c	P_r^d
1	5	100/1	15	54.8	7.90	10.8	1.39	0.53
2	5	100/1	60	74	10.7	12.7	1.67	0.53
3	5	100/1	120	91.1	13.2	20.2	1.65	0.51
4	6	100/1	15	41.4	4.72	1.28	1.18	0.53
5	6	100/1	60	83.9	9.58	3.39	1.54	0.53
6	6	100/1	120	95.2	10.9	3.96	1.66	0.53

^aDetermined from ¹H NMR. ^b $M_{n\text{cal}}$ of polymer calculated from $M_n = ([\text{rac-LA}]_0/[\text{Zn}]_0) \times 144.13 \times \text{conversion (\%)} / 100$. ^cDetermined by GPC (chloroform), relative to polystyrene standards. The M_n was calculated according to $M_n = 0.58M_{n\text{GPC}}$. ^d P_r is the probability of racemic enchainment of monomers units, determined by homodecoupled ¹H NMR spectra according to Coates *et al.*^[51]

Table 3. Ring-opening polymerization of ϵ -caprolactone initiated by complexes **2-5** and **7** in toluene

Entry	Initiator	$[\epsilon\text{-CL}]_0/[\text{Zn}]_0/[\text{ROH}]_0$	t /min	T °C	Conv. (%) ^d	$M_{\text{ncal}}^e \times 10^3$	$M_n^f \times 10^3$	M_w/M_n^f
1	2	100/1/1 ^b	15	60	74.4	8.49	5.69	1.27
2	2	200/1/1 ^b	60	60	94.5	21.4	9.72	1.34
3	3	100/1/1 ^a	120	70	17.1	-	-	-
4	3	200/1/1 ^a	270	70	76.3	17.4	14.6	1.82
5	3	100/1/1 ^a	5	130 ^c	50.0	5.71	12.2	1.37
6	3	100/1/1 ^b	5	130 ^c	98.3	11.2	7.70	1.46
7	4	100/1/1 ^b	40	70	99	11.3	8.56	1.22
8	5	100/1/0	60	70	95	10.8	9.03	1.30
9	7	100/1/1 ^b	30	70	88.5	20.2	17.5	1.21

^aIn presence of one equivalent of *tert*-butyl alcohol. ^bIn presence of one equivalent of benzyl alcohol. ^cMicrowave reaction (MW). ^dDetermined from ¹H NMR. ^e M_{ncal} of polymer calculated from $M_{\text{ncal}} = ([\epsilon\text{-CL}]_0/[\text{Zn}]_0) \times 114.14 \times \text{conversion (\%)} / 100$. ^f M_n^{GPC} was determined by GPC (chloroform), relative to polystyrene standards. M_n was corrected according to $M_n = 0.56M_n^{\text{GPC}}$

Ring-opening polymerization of ϵ -caprolactone

Polymerization of ϵ -caprolactone by complexes **2-5** and **7** was also assessed (Table 3). Similar trends in behaviour can be seen when compared with ROP of *rac*-lactide, e.g. slow initiation and reaction rate when *t*BuOH was used as co-initiator (entries 3 and 4). Molecular weight distributions were between 1.22 and 1.82. Conversions were generally higher when BnOH, which is less sterically demanding, was used. The *t*-Am substituted ligands afforded initiators with the greatest degree of reaction control for ROP of ϵ -caprolactone, in that **4** and **5** afforded P(ϵ -CL) with narrow molecular weight distributions and molecular weights close to the expected values (Table 3, entries 7 and 8).

Reactivity of complexes towards CO₂ and cyclohexene oxide

Amongst catalytic coordination complexes for CO₂/epoxide couplings and copolymerizations, zinc is central to many of the species studied.^[29,30,52-55] Therefore, studies were performed using **6** and **7**/ROH in combination with DMAP and Bu₄NBr as co-catalysts, Table 4, towards the reaction of CO₂ with cyclohexene oxide. A control reaction was performed using Bu₄NBr alone, as ionic salts such as this are known to catalyze the formation of cyclic carbonates (Table 4, entry 1).^[56-57] Compounds **6** and **7** exhibit some activity towards cyclic carbonate formation under high temperature and pressure conditions in the presence of an ionic co-catalyst. Comparison of entries 1 and 5 indicates that the zinc complex does play a role in this reaction as the conversion has increased by 18.1% and a small amount of *trans*-cyclic carbonate was observed. **7**/EtOH/Bu₄NBr under the same conditions, entry 7, produced slightly less carbonate but with a larger amount of the *trans*-isomer. The *cis*- and *trans*-isomers are likely formed through different mechanisms with the *trans*-isomer probably formed through a back-biting reaction at the metal centre. Although conversions were modest and high temperatures and pressures were required, compared to state-of-the-art catalysts in the literature, these results can act as a starting point for further studies and also give some indication of the reason for CO₂ uptake by the related Zn complexes used by Lappert and co-workers.^[26]

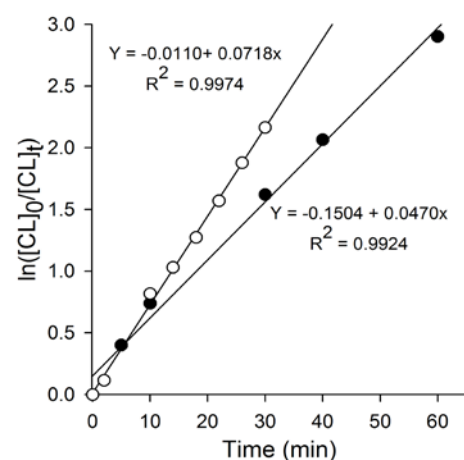


Figure 10. First-order plots of ϵ -CL consumption at 70 °C using **7**/BnOH (hollow circles) and **2**/BnOH (filled circles). Conditions: $[\epsilon\text{-CL}]:[\text{Zn}] = 200:1$, 1 equiv. BnOH, $[\text{Zn}]_0 = 22.5$ mM (**7**) and 18.8 mM (**2**).

Table 4. Reactions of cyclohexene oxide (CHO) with CO₂ in the presence of Zn complexes and co-catalysts

Entry	Catalyst	Co-catalyst	[CHO] ₀ /[Zn] ₀ /[Co-cat] ₀	t (h)	P (bar)	T (°C)	Conv. (%) ^a
1	-	Bu ₄ NBr	500/0/1	24	65	100	39.0 (100% <i>cis</i>)
2	6	-	500/1/0	18	45	70	0
3	6	DMAP	500/1/1	16	45	70	0
4	6	Bu ₄ NBr	500/1/1	18	45	70	4.8
5	6	Bu ₄ NBr	500/1/1	24	65	100	57.1 (96.2% <i>cis</i>)
6	7 + BnOH	Bu ₄ NBr	500/1/1	18	45	70	8.3
7	7 + EtOH	Bu ₄ NBr	500/1/1	24	65	100	45.1 (86.4% <i>cis</i>)

^aDetermined by relative intensities of the methine protons via ¹H NMR.^[58]

Conclusions

Piperazinyl-derived amine-phenolate protio ligands can be prepared in excellent yields in water *via* a modified Mannich-condensation reaction. As expected, these ligands readily react with diethyl zinc and generally afford phenolate bridged Zn-Et dimers. These complexes readily undergo alcoholysis reactions to yield alkoxide bridged species. A range of these complexes has been structurally characterized. The Zn-Et species in the presence of an alcohol and the alkoxide complexes as single-component initiators are able to facilitate ring-opening polymerization of cyclic esters, however, no control of stereoselectivity is observed in ROP of *rac*-lactide and this is likely due to the solvent employed. In comparison with morpholinyl-derived complexes, the piperazinyl-derived species show slower reaction rates. MW irradiation was used in some of the ROP reactions and was useful in reducing reaction times whilst maintaining control of the reaction (*i.e.* increased polydispersities, due to the higher temperature used, were not observed). Both classes of complex show slight activity towards cyclic carbonate formation from cyclohexene oxide and carbon dioxide. These studies suggest that an outer-sphere ligand group or base (ether or amine) within an initiating or catalytic species can affect the outcome of ROP and potentially other reactions. Further studies utilizing these interesting ligands are underway in our laboratory.

Experimental Section

General Considerations

All experiments involving metal complexes were performed under a nitrogen atmosphere using standard Schlenk and glove-box techniques. THF was distilled under nitrogen over sodium/benzophenone. Toluene and hexane were purified by an MBraun Solvent Purification System. Deuterated solvents (C₆D₆, CDCl₃, C₅D₅N) were purchased from Cambridge Isotope Laboratories, Inc. and purified and dried before use. All solvents were degassed by freeze-vacuum-thaw cycles prior to use. 2,4-

di(*tert*-butyl)phenol, 2-*tert*-butyl-4-methylphenol, 2,4-di(*tert*-amyl)phenol, *n*-butyl lithium, 1-methyl piperazine, morpholine, diethyl zinc (15 wt% solution in hexane), *rac*-lactide, ε-caprolactone and cyclohexene oxide were purchased from Sigma-Aldrich or Alfa Aesar. Monomers were dried and degassed prior to use. Elemental analyses were performed by Canadian Microanalytical Service Ltd., Delta, BC, Canada. ¹H and ¹³C{¹H} NMR spectra were recorded on a Bruker Avance 500 MHz spectrometer at 25 °C (unless otherwise stated) and were referenced internally using the residual proton and ¹³C resonances of the solvent. ¹³C signals were assigned using HSQC experiments. MALDI-TOF MS was performed using an Applied Biosystems Voyager DE-PRO equipped with a reflectron, delayed ion extraction and high performance nitrogen laser (337 nm). Anthracene was used as the matrix for ligands and complexes.^[59-60] Mass spectra were also obtained by AP-CI MS in positive mode (70 eV) using an Agilent 1100 LC mass spectrometer. GPC data were collected on a Viscotek GPCMax System equipped with a Refractive Index Detector and columns purchased from Phenomenex (Phenogel 5 μ Linear/mixed bed 300 × 4.60 mm column in series with a Phenogel 5 μ 100 Å 300 × 4.60 mm column). Samples were run in chloroform at 35 °C at a concentration of 1 mg/mL. The instrument was calibrated against polystyrene standards (Viscotek) to determine the molecular weights (M_n and M_w) and the polydispersity index (M_w/M_n) of polymers. For PLA samples, P_r (the probability of racemic enchainment) was determined by analysis of the methine region of the homonuclear decoupled ¹H NMR spectra (CDCl₃). The equations used to calculate P_r were as described by Coates *et al.*^[51] The conversions were determined by ¹H NMR integration of the OCHMe resonance relative intensities of the residual *rac*-lactide and poly(*rac*-lactide) and integration of the ε-methylene of residual ε-caprolactone and poly(ε-caprolactone).

Microwave-heated polymerizations were performed using a Biotage InitiatorTM eight microwave synthesizer.

Crystallographic procedures

All crystals were mounted on a low temperature diffraction loop in paratone oil. Measurements were made on a Rigaku AFC8-Saturn 70 single crystal X-ray diffractometer equipped with an X-stream 2000 low temperature system and a SHINE optic, using Mo-K α radiation. Data were collected and processed using CrystalClear (Rigaku).^{61a} Numerical absorption corrections were applied and the data were corrected for Lorentz and polarization effects. The structures were solved by direct methods (**L1H**, **1**, **3**, **4**, **5**, **6**, **7**),^{61b} (**2**)^{61c} and expanded using Fourier techniques.^{61d} Neutral atom scattering factors were taken from Cromer and Waber.^{61e} Anomalous dispersion effects were included in Fcalc;^{61f} the values for Δf and $\Delta f''$ were those of Creagh and McAuley.^{61g} The values for the mass attenuation coefficients were those of Creagh and Hubbell.^{61h} All calculations were performed using the CrystalStructure^{61i,j} crystallographic software package except for refinement, which was performed using SHELXL-97.^{61b} Hydrogen atoms were introduced in calculated positions and refined on a riding model, unless otherwise indicated, while all non-hydrogen atoms were refined anisotropically.

For **L2H**, **1**, **3**, **5** and **6**, collection, solution and refinement proceeded normally. For **L2H**, H1 was introduced in its difference map position and was refined initially on (x,y,z), and finally on a riding model. Friedel mates were averaged and the absolute configuration was not determined. The asymmetric unit of **1** contained a half-occupancy toluene molecule that was disordered over two sites. The corresponding protons could not be located from difference maps, and were omitted from the model. For **5**, one disordered amyl group was present (PART 1 – [C32-35, C39] at 0.65 occupancy; PART 2 – [C32A, C36-38, C40] at 0.35 occupancy). Hydrogen atoms on C33 and C36 were omitted from the model.

2 and **7** were refined as non-merohedral twins with component #1 comprising 47.99% and 64.81% of the crystal respectively. For **2**, a large negative residual density was present (1.82 Å from H5A) likely resulting from twinning which was not allowed for, where overlap from the second twin domain caused errors in the intensities of some reflections. **4** was refined as a merohedral twin, with component #1 comprising 19.60% of the crystal. The merohedral twin law was identified using Platon's TwinRotMat.^{61k}

Crystallographic data for this paper can be obtained free of charge from The Cambridge Crystallographic Data Centre via www.ccdc.cam.ac.uk/data_request/cif. CCDC-762217 (for **L2H**), -762221 (for **1**), -762220 (for **2**), -762222 (for **3**), -833271 (for **4**), -762223 (for **5**), -833272 (for **6**), -833273 (for **7**).

Synthetic Procedures

L1H. Water (80 mL), 2-*tert*-butyl-4-methylphenol (10.10 g, 61.5 mmol) and formaldehyde, 37% solution in water, (5 mL, 61.5 mmol) were added to 250 mL round-bottom flask equipped with a stir bar and a condenser. 1-methyl piperazine (6.8 mL, 61.5 mmol) was added dropwise to the stirred solution. The resulting mixture was heated at reflux for 18 h. Upon cooling to room temperature, a two phase mixture was formed. The organic layer (solid) was isolated, washed with methanol and dried under vacuum to remove any unreacted organic components. The resulting pale-gray solid was recrystallized in methanol to give colorless crystals. Yield: 16.71 g, 98%. mp 90 °C; MS (AP-CI, solvent: MeOH) m/z 277 (M $^+$, 100%); Anal. Calc. for C₁₇H₂₈N₂O: C, 73.87; H, 10.21; N, 10.13. Found: C, 73.81; H, 10.10; N, 10.66; ¹H NMR (CDCl₃, 500 MHz, 298 K) δ 10.90 (1H, s, ArOH), 6.99 (1H, s, ArH), 6.67 (1H, s, ArH), 3.65 (2H, s, Ar-CH₂-N), 2.51 (8H, br, NCH₂CH₂N), 2.31 (3H, s, NCH₃), 2.23 (3H, s, ArCCH₃) 1.40 (9H, s, ArC-C(CH₃)₃): ¹³C{¹H} NMR (CDCl₃, 125 MHz, 298 K): δ 154.7 (ArC-OH), 136.6 (ArC-CH₂-N), 127.7 (ArCH), 127.5 (ArCH), 127.0 (ArC-C(CH₃)₃), 121.6 (ArCCH₃), 62.1 (ArC-CH₂-N), 55.3 (N-CH₂-CH₂-N), 52.7 (N-CH₂-CH₂-N), 46.3 (CH₃-N), 35.0 (ArC-C(CH₃)₃), 30.0 (ArC-C-(CH₃)₃), 21.2 (ArC-CH₃).

L2H. This compound was prepared in the same manner as described above for **L1H** with 2,6-di-*tert*-butylphenol (12.69 g, 61.5 mmol), formaldehyde, 37% solution in water (5 mL, 61.5 mmol), and 1-methyl piperazine (6.8 mL, 61.5 mmol) as starting materials. The product was recrystallized to yield a colorless crystalline solid. Yield: 17.65 g, 90%. mp 119 °C; MS (MALDI, matrix: anthracene) m/z 381 (M $^+$, 100%); Anal. Calc. for C₂₀H₃₄N₂O: C, 75.42; H, 10.76; N, 8.80. Found: C, 75.40; H, 10.65; N, 8.79. ¹H NMR (CDCl₃, 500 MHz, 298 K) δ 11.49 (1H, s, ArOH), 7.26 (1H, s, ArH), 6.93 (1H, s, ArH), 3.75 (2H, s, Ar-CH₂-N), 2.98 (4H, d, J = 10.2, NCH₂CH₂N), 2.86 (4H, d, J = 10.3, NCH₂CH₂N), 2.35 (3H, s, NCH₃), 1.42 (9H, s, C(CH₃)₃), 1.29 (9H, s, C(CH₃)₃): ¹³C{¹H} NMR (CDCl₃, 125 MHz, 298 K): δ 154.5 (ArCOH), 140.9 (ArCC(CH₃)₃), 135.8 (ArC-C(CH₃)₃), 123.8 (ArCH), 123.3 (ArCH), 120.9 (ArC-CH₂), 62.5 (CH₃-N), 55.3 (N-CH₂-CH₂-N), 52.7 (N-CH₂-CH₂-N), 46.3 (ArC-C-CH₂), 35.2 (ArC-C(CH₃)₃), 34.5 (ArC-C(CH₃)₃), 32.1 (ArC-C-(CH₃)₃), 30.0 (ArC-C-(CH₃)₃).

L3H. Water (100 mL), 2,6-di-*tert*-amylphenol (18.99 g, 81.0 mmol) and formaldehyde, 37% solution in water, (6.6 mL, 81.0 mmol) were added to a 500 mL round-bottom flask equipped with a stir bar and a condenser. 1-Methyl piperazine (8.1 g, 81.0 mmol) was added dropwise to the stirred solution. The resulting mixture was heated at reflux for 18 h. Upon cooling to room temperature, a two phase mixture formed. The organic material was extracted with diethyl ether and dried over magnesium sulfate. The solvent was removed by rotary evaporation to give a pale-brown oil from which colorless crystals were obtained upon standing for several days under ambient conditions. Yield: 23.02 g, 82%. mp 82 °C; MS (AP-CI, solvent: MeOH) m/z 347 (M $^+$, 100%); Anal. Calc for C₂₂H₃₈NO₂: C, 76.25; H, 11.05; N, 8.08. Found: C, 76.36; H, 10.80; N, 8.04. ¹H NMR (CDCl₃, 500 MHz, 298 K) δ 10.77 (1H, s, ArOH), 7.07 (1H, d, J = 2.2 Hz, ArH), 6.75 (1H, d, J = 2.2 Hz, ArH), 3.67 (2H, s, ArC-CH₂-N), 2.53 (8H, br, N-C₂H₄-N), 2.30 (3H, s, NCH₃), 1.88 (2H, q, J = 7.4 Hz, CCH₂CH₃), 1.56 (2H, q, J = 7.4 Hz, CCH₂CH₃), 1.36 (6H, s, ArC-C(CH₃)₂), 1.23 (6H, s, ArC-C(CH₃)₂), 0.65 (3H, t, J = 7.4 Hz, CH₂CH₃), 0.64 (3H, t, J = 7.4 Hz, CH₂CH₃). ¹³C{¹H} NMR (CDCl₃, 500 MHz, 298 K): δ 154.2 (ArC-OH), 139.0 (ArCC(CH₃)₃), 134.1 (ArC-C(CH₃)₃), 125.3 (ArCH), 124.4 (ArCH), 120.6 (ArC-CH₂-N), 62.5 (N-CH₂-C), 55.3 (N-CH₂-CH₂-N), 52.3 (N-CH₂-CH₂-N), 46.3 (ArC-C(CH₃)₂-CH₂), 38.7 (N-CH₃), 37.6 (C(CH₃)₂-CH₂), 37.5 (C(CH₃)₂-CH₂), 33.4 (ArC-C(CH₃)₂-CH₂), 28.9 (C(CH₃)₂-CH₂), 28.0 (C(CH₃)₂-CH₂), 9.8 (CH₂-CH₃), 9.5 (CH₂-CH₃).

L4H. Water (80 mL), 2-*tert*-butyl-4-methylphenol (16.51 g, 80.0 mmol) and formaldehyde, 37% solution in water, (6.50 mL, 80.0 mmol) were added to 250 mL round-bottom flask equipped with a stir bar and a condenser. Morpholine (6.97 mL, 80.0 mmol) was added dropwise to the stirred solution. The resulting mixture was heated at reflux for 18 h. Upon cooling to room temperature, a two phase mixture was formed. The organic layer (solid) was isolated, washed with methanol and dried under vacuum to remove any unreacted organic components. The resulting brown gel-like solid was recrystallized in methanol to give a colorless solid. Yield: 21.23 g, 87%. mp 112 °C; MS (MALDI, matrix: anthracene) m/z 305 (M $^+$, 100%); Anal. Calc. for C₁₉H₃₁NO₂: C, 74.71; H, 10.23; N, 4.59. Found: C, 74.66; H, 10.27; N, 4.52. ¹H NMR (CDCl₃, 500 MHz, 298 K) δ 10.66 (1H, s, ArOH), 7.23 (1H, d, J = 2.2 Hz, ArH), 6.84 (1H, d, J = 2.2 Hz, ArH), 3.75 (2H, s, Ar-CH₂-N), 3.68 (4H, br, OC₂H₄C₂H₄N) 2.56 (4H, br, OC₂H₄C₂H₄N), 1.41 (9H, s, C(CH₃)₃), 1.28 (9H, s, C(CH₃)₃). ¹³C{¹H} NMR (CDCl₃, 125 MHz, 298 K): δ 154.4 (ArC-OH), 141.2 (ArC-C(CH₃)₃), 136.0 (ArC-C(CH₃)₃), 124.0 (ArCH), 123.6 (ArCH), 120.5 (ArC-CH₂), 67.2 (O-C₂H₄-C₂H₄-N), 63.1 (ArCCH₂N), 53.2 (O-C₂H₄-C₂H₄-N), 35.3 (ArC-C(CH₃)₃), 34.6 (ArC-C(CH₃)₃), 32.1 (ArC-C-(CH₃)₃), 30.0 (ArC-C-(CH₃)₃).

Zn[ONN^{tBu,tBu}]₂ (1). This compound was prepared in the same manner as described below for **2** with diethylzinc (1.7 mL, 2.0

mmol; 15 wt% in hexane) and **L2H** (0.64 g, 2.0 mmol) as starting materials. **1** was obtained as a colorless crystalline solid. Yield: 1.07 g, 77%. Crystals suitable for X-ray crystallography could be grown by slow evaporation or by cooling a saturated toluene/hexane solution at -35 °C. Anal. Calc for C₄₇H₇₄N₄O₂Zn(C₇H₈): C, 71.23; H, 9.41; N, 7.07. Found: C, 71.10; H, 9.49; N, 7.05. ¹H NMR (C₅D₅N, 500 MHz, 343K) δ 7.58 (1H s, ArH), 7.11 (1H, s, ArH), 4.07 (2H, s, Ar-CH₂-N), 3.07 (4H, br, NCH₂CH₂N), 2.83 (4H, s, NCH₂CH₂N), 2.29 (3H, s, NCH₃), 1.60 (9H, s, C{CH₃}₃), 1.44 (9H, s, C{CH₃}₃), ¹³C{¹H} NMR (C₅D₅N, 125 MHz, 298 K): δ 165.3 (ArC-O), 137.8 (ArC-CH₂N), 134.5 (ArC C{CH₃}₃), 129.6 (CH), 128.9 (CH), 122.1 (ArC-C{CH₃}₃), 64.6 (ArCCH₂N), 55.1 (N-CH₂-CH₂-N), 53.5 (N-CH₂-CH₂-N), 46.1 (CH₃-N), 36.0 (ArC-C{CH₃}₃), 34.4 (ArC-C{CH₃}₃), 32.6 (C{CH₃}₃), 30.5 (C{CH₃}₃).

{[μ-ONN^tBu,^tBu]ZnEt}₂ (**2**). To a 50 mL flask containing diethylzinc (6.2 mL, 5.02 mmol; 15 wt% in hexane) was added dropwise a solution of **L1H** (1.39 g, 5.02 mmol) in toluene (2.0 mL) cooled to -35 °C. The colorless mixture was allowed to warm with stirring to room temperature for 18 h. Volatiles were removed under vacuum to give a white residue, which was washed with hexane (2 × 4 mL) and dried *in vacuo*. The crude product was recrystallized from a saturated toluene solution at -35 °C to give **2** as a colorless crystalline solid. Yield: 1.43 g, 77%. Anal. Calc for C₃₈H₆₄N₄O₂Zn₂: C, 61.70; H, 8.72; N, 7.57. Found: C, 62.02; H, 9.13; N, 7.98; ¹H NMR (C₅D₅N, 500 MHz, 343 K) δ 7.33 (1H s, ArH), 6.84 (1H, s, ArH), 4.00 (2H, s, Ar-CH₂-N), 3.04 (4H, br, N CH₂CH₂N), 2.83 (4H, br, NCH₂CH₂N), 2.35 (3H, s, NCH₃), 2.30 (3H, s, ArC-CH₃), 1.78 (2H, s, CH₂CH₃), 1.58 (9H, q, ArC-C{CH₃}₃), 0.91 (3H, t, CH₂CH₃). ¹³C{¹H} NMR (C₅D₅N, 125 MHz, 298 K): δ 164.4 (ArC-O), 138.6 (C-CH₂N), 130.4 (ArCH), 128.7 (ArCH), 121.9 (C-C{CH₃}₃), 120.8 (C{CH₃}), 64.6 (N-CH₂-C), 55.4 (N-CH₂-CH₂-N), 53.0 (N-CH₂-CH₂-N), 45.9 (Ar-CH₂-N), 35.5, (CH₃-N), 30.6 (C{CH₃}₃), 30.4 (C{CH₃}₃), 21.4 (CH₃CH₂), 21.2 (C{CH₃}), 14.1 (CH₃CH₂).

{[μ-ONN^tBu,^tBu]ZnEt}₂ (**3**). To a 50 mL flask containing diethylzinc (3.3 mL, 4.0 mmol; 15 wt% in hexane) was added dropwise a solution of **L2H** (0.64 g, 2.0 mmol) in toluene (2.0 mL) cooled to -35 °C. The colorless mixture was allowed to warm with stirring to room temperature for 18 h. Volatiles were removed under vacuum to give a white residue, which was washed with hexane (2 × 4 mL) and dried *in vacuo*. Yield: 0.92 g, 56%. Crystals suitable for X-ray crystallography could be grown by slow evaporation or by cooling a saturated toluene/hexane solution at -35 °C. Anal. Calc. for C₄₄H₇₆N₄O₂Zn₂: C, 64.14; H, 9.30; N, 6.80. Found: C, 63.72; H, 9.21; N, 6.10. ¹H NMR (C₅D₅N, 500 MHz, 358 K) δ 7.63 (1H s, ArH), 7.10 (1H, s, ArH), 3.65 (2H, s, Ar-CH₂-N), 2.64 (4H, br, NCH₂CH₂N), 2.54 (4H, s, NCH₂CH₂N), 2.27 (3H, s, NCH₃), 1.81 (9H, s, C{CH₃}₃), 1.57 (3H, t, J = 8.0 Hz, CH₃CH₂), 1.50 (9H, s, C{CH₃}₃), 0.59 (2H, q, J = 8.0 Hz, CH₃CH₂). ¹³C{¹H} NMR (C₅D₅N, 125 MHz, 298 K): δ 165.3 (ArC-O), 138.3 (ArC-CH₂N), 134.5 (ArC-C{CH₃}₃), 126.6 (ArCH), 126.0 (ArCH), 122.1 (ArC-C{CH₃}₃), 64.6 (ArC-CH₂-N), 55.2 (N-CH₂-CH₂-N), 53.5 (N-CH₂-CH₂-N), 46.1 (CH₃-N), 36.0 (C{CH₃}₃), 34.4 (C{CH₃}₃), 32.6 (C{CH₃}₃), 30.5 (C{CH₃}₃), 14.1 (CH₃CH₂), 1.5 (CH₃CH₂).

{[μ-ONN^tAm,^tAm]ZnEt}₂ (**4**). To a 50 mL flask containing diethylzinc (6.2 mL, 5.02 mmol; 10 wt% in hexane) was added dropwise a solution of **L3H** (1.74 g, 5.02 mmol) in toluene (2.0 mL) cooled to -35 °C. The colorless mixture was allowed to warm with stirring to room temperature for 18 h. Volatiles were removed under vacuum to give a white residue, which was washed with hexane (2 × 4 mL) and dried *in vacuo*. The crude product was recrystallized from a saturated toluene solution at -35 °C to give {[μ-ONN^tAm,^tAm]ZnEt}₂ as a colorless crystalline solid. Yield: 1.92 g, 87%. Anal. Calc for C₄₈H₈₄N₄O₂Zn₂: C, 65.51; H, 9.62; N, 6.37. Found: C, 65.47; H, 10.89; N, 6.28. ¹H NMR (C₅D₅N, 500 MHz,

358 K) δ 7.49 (1H, s, ArH), 7.04 (1H, s, ArH), 3.65 (2H, s, ArC-CH₂-N), 2.64 (4H, br, NCH₂CH₂N), 2.56 (4H, s, NCH₂CH₂N), 2.41 (2H, q, J = 7.4 Hz, CCH₂CH₃), 2.27 (3H, s, NCH₃), 1.80 (2H, q, J = 7.4 Hz, CCH₂CH₃), 1.74 (6H, s, C(CH₃)₂), 1.59 (3H, t, J = 8.0 Hz, CH₃CH₂), 1.46 (6H, s, C(CH₃)₂), 0.98 (3H, t, J = 7.4 Hz, CH₂CH₃), 0.91 (3H, t, J = 7.4 Hz, CH₂CH₃), 0.61 (2H, q, J = 8.0 Hz, CH₃CH₂). ¹³C{¹H} NMR (C₅D₅N, 125 MHz, 298 K): δ 165.2 (ArC-O), 132.4 (ArC-CH₂-N), 127.3 (ArCH), 126.4 (ArCH), 121.8 (ArC-C{CH₃}₂-CH₂]), 64.5 (ArC-CH₂-N), 55.1 (N-CH₂-CH₂-N), 53.5 (N-CH₂-CH₂-N), 46.1(N-CH₃), 39.42 (C{CH₃}₂-CH₂]), 37.9 (C{CH₃}₂-CH₂]), 37.5 (C{CH₃}₂-CH₂]), 33.3 (C{CH₃}₂-CH₂]), 29.6-28.5 (C{CH₃}₂-CH₂]), 14.1 (CH₃CH₂) 10.7-9.9 ({CH₃}₂-CH₂-CH₃), 1.6 (CH₃CH₂).

{[ONN^tAm,^tAm]Zn(μ-OBn)}₂ (**5**). To a solution of **4** (0.80 g, 0.91 mmol) in toluene (5 mL) cooled to -35 °C was added BnOH (190 μL, 1.8 mmol) dropwise. The reaction mixture was allowed to warm with stirring to room temperature for 3 h. The solvent was removed under vacuum to give a white residue, which was washed with cold hexane (2 × 4 mL) and dried *in vacuo*. The crude product was recrystallized from toluene/hexane to give the product {[ONN^tAm,^tAm]Zn(μ-OBn)}₂ as a colorless crystalline solid. Yield: 0.84 g, 89%. Anal. Calc for C₅₈H₈₈N₄O₄Zn₂: C, 67.23; H, 8.56; N, 5.41. Found: C, 67.78; H, 9.12; N, 5.63. ¹H NMR (C₅D₅N, 500 MHz, 343 K) δ 7.69 (1H, s, ArH), 7.51 (2H, s, ArH), 7.43 (1H, s, ArH), 7.37 (1H, s, ArH), 7.05 (2H, s, ArH), 5.11 (2H, br, OCH₂Ar), 4.09 (2H, s, ArC-CH₂-N), 2.60-3.05 (8H, br, overlapping, N-C₂H₄-N), 1.77 (4H, m, CCH₂CH₃), 1.58 (3H, s, NCH₃), 1.41 (6H, s, C(CH₃)₂), 1.38 (6H, s, C(CH₃)₂), 0.87 (6H, m, CH₂CH₃). ¹³C{¹H} NMR (C₅D₅N, 125 MHz, 298 K): δ 163.8 (ArC-O), 144.5 (ArC-CH₂), 133.6 (ArC-CH₂-N), 129.1 (ArC), 129.0 (ArC), 128.0 (ArCH), 127.3 (ArCH), 126.8 (ArC), 119.9 (ArC-C{CH₃}₂-CH₂]), 69.4 (ArC-CH₂), 65.0 (ArC-CH₂-N), 55.3 (N-CH₂-CH₂-N), 54.2 (N-CH₂-CH₂-N), 45.9 (N-CH₃), 39.1 (C{CH₃}₂-CH₂]), 37.8 (C{CH₃}₂-CH₂]), 37.5 (C{CH₃}₂-CH₂]), 33.4 (C{CH₃}₂-CH₂]), 29.4 - 28.5 (C{CH₃}₂-CH₂]), 10.4-9.9 ({CH₃}₂-CH₂-CH₃).

{[ONN^tBu,^tBu]Zn(μ-OEt)}₂ (**6**) To a 50 mL flask containing diethylzinc (7.8 mL, 6.3 mmol; 15 wt% in hexane) was added dropwise a solution of **L2H** (2.00 g, 6.3 mmol) in cooled toluene (2.0 mL) at -35 °C. The colorless mixture was allowed to warm with stirring to room temperature for 3 h. Volatiles were removed under vacuum to give an off-white residue, which was washed with pentane (2 × 4 mL) and redissolved in toluene (2.0 mL). To this solution was added EtOH (366 μL, 6.3 mmol) dropwise and the reaction mixture was allowed stirring at room temperature for 18 h. The resulting mixture was filtered and the filtrate was concentrated under vacuum and cooled at -35 °C to afford **6** as a colorless crystalline solid. Yield: 1.65 g, 61%. Anal. Calc for C₄₄H₇₆N₄O₄Zn₂: C, 61.75; H, 8.95; N, 6.55. Found: C, 61.69; H, 9.19; N, 7.00. ¹H NMR (C₅D₅N, 500 MHz, 358 K) δ 7.72 (1H s, ArH), 7.66 (1H, s, ArH), 4.04 (2H, br, OCH₂CH₃), 3.83 (2H, s, Ar-CH₂-N), 3.00 (4H, br, NCH₂CH₂N), 2.79 (4H, br, NCH₂CH₂N), 2.53 (3H, s, NCH₃), 1.92 (9H, s, C{CH₃}₃), 1.58 (9H, s, C{CH₃}₃), 1.55 (3H, t, OCH₂CH₃). ¹³C{¹H} NMR (C₅D₅N, 125 MHz, 298 K): δ 164.2 (ArC-O), 138.1 (C-CH₂N), 126.4 (ArCH), 126.1 (ArCH), 119.9 (C-C{CH₃}₃), 119.7 (C-C{CH₃}₃), 65.6 (N-CH₂-C), 55.3 (N-CH₂-CH₂-N), 54.1 (N-CH₂-CH₂-N), 46.1 (CH₃-N), 45.8(OCH₂CH₃) 36.0 (C{CH₃}₃), 35.6 (C{CH₃}₃), 34.3 (OCH₂CH₃) 32.4 (C{CH₃}₃), 30.5 (C{CH₃}₃).

{[μ-ONO^tBu,^tBu]ZnEt}₂ (**7**). To a 50 mL flask containing diethylzinc (6.2 mL, 5.02 mmol; 15 wt% in hexane) was added dropwise a solution of **L4H** (1.53 g, 5.02 mmol) in cooled toluene (2.0 mL) at -35 °C. The colorless mixture was allowed to warm with stirring to room temperature for 18 h. Volatiles were removed under vacuum to give a white residue, which was washed with hexane (2 × 4 mL) and dried *in vacuo*. Yield: 1.62 g, 81%. Crystals suitable for X-ray crystallography could be grown by slow

evaporation or by cooling a saturated toluene solution at -35 °C. Anal. Calc for C₄₂H₇₀N₄O₄Zn₂C, 63.23; H, 8.84; N, 3.51. Found: C, 63.16; H, 8.55; N, 3.60. ¹H NMR (C₅D₅N, 500 MHz, 313 K) δ 7.63 (1 H, s, ArH), 7.10 (1 H, s, ArH), 3.81 (4H, br, OC₂H₄C₂H₄N), 3.59 (2H, s, Ar-CH₂-N), 2.50 (4H, br, OC₂H₄C₂H₄N), 1.79 (9H, s, C(CH₃)₃), 1.59 (3H, t, J = 8.0 Hz, CH₃CH₂), 1.48 (9H, s, C(CH₃)₃), 0.58 (2H, q, J = 8.0 Hz, CH₃CH₂). ¹³C{¹H} NMR (C₅D₅N, 125 MHz, 298 K): δ 165.35 (ArC-O), 141.2 (ArC-C(CH₃)₃), 137.93 (ArC-CH₂N), 134.70 (ArC-C(CH₃)₃), 126.73 (ArCH), 124.44 (ArCH), 121.57 (ArC-C(CH₃)₃), 65.55 (O-C₂H₄-C₂H₄-N), 65.45 (O-C₂H₄-C₂H₄-N), 65.13 (ArCCH₂N), 36.01 (ArC-C(CH₃)₃), 34.41 (ArC-C(CH₃)₃), 32.60 (ArC-C(CH₃)₃), 30.48 (ArC-C(CH₃)₃), 13.98 (CH₃CH₂), 0.76 (CH₃CH₂).

Typical solution polymerization procedure. The reaction mixtures were prepared in a glove-box and subsequent operations were performed using standard Schlenk techniques. A monomer:initiator ratio of 100:1 was employed. To a sealable Schlenk tube with a stir bar containing the monomer (0.05 mmol) in toluene (8.00 mL) heated to the desired temperature, was added initiator solution (26.3 mM) from a stock solution containing a prescribed amount of ROH. The mixture was stirred for the allotted time. An aliquot of the reaction sample was taken for NMR spectroscopic analysis and the reaction was quenched immediately by addition of methanol. The resulting solid was dissolved in dichloromethane and the polymer precipitated with excess cold methanol. The polymer was collected by filtration, washed with methanol to remove any unreacted monomer and dried under reduced pressure.

Bulk polymerization. For solvent-free polymerizations of *rac*-lactide, the monomer:initiator ratio employed was 100:1 at a temperature of 130 °C. A Schlenk tube equipped with magnetic stir bar was charged in the glovebox with the required amount of *rac*-lactide (0.50 g, 3.5mmol) and initiator (0.042 - 0.015 g). The reaction vessel was sealed, brought out of the glove-box and immersed in an oil bath preheated to 130 °C. At the desired time an aliquot, *ca* 0.3 mL was withdrawn from the flask for ¹H NMR analysis to determine monomer conversion. The reaction was quenched with methanol and the resulting solid was dissolved in dichloromethane, precipitated with excess cold methanol, filtered and dried under reduced pressure.

Typical microwave-assisted ring-opening polymerization.

To a microwave vial charged with lactide (576 mg, 5.27 mmol) or ε-caprolactone (601 mg, 5.27 mmol) in toluene (10 mL), was added a toluene solution (2.00 mL) of the initiator containing a prescribed amount of benzyl or *tert*-butyl alcohol. The vial was sealed with a septum and the mixture was irradiated to a constant required temperature for the desired amount of time. After irradiation, the vial was cooled to room temperature, an aliquot of the product was taken for NMR spectroscopic analysis and the reaction was quenched immediately by addition of methanol. The resulting solid was dissolved in dichloromethane and the polymer precipitated with excess cold methanol. A colorless product was collected by filtration, washed with methanol to remove any unreacted monomer and dried under reduced pressure.

CO₂-cyclohexene oxide reactions. The complex (0.2 mol%) was dissolved in cyclohexene oxide (2.27 g, 23.2 mmol) in the glovebox. The mixture and co-catalyst (0.2 mol%) was placed in a predried autoclave equipped with a pressure gauge. The autoclave was sealed, removed from the glovebox and attached to an overhead magnetic stirrer. The system was pressurized to approx.

40 bar with CO₂ and heated.[§] The mixture was stirred for the desired time and then the pressure was slowly released whilst cooling the pressure vessel in an ice-bath. A small amount of the residue in the vessel was removed for ¹H NMR analysis

Supporting Information (see footnote on the first page of this article): ¹H NMR and MALDI-TOF MS spectra of L2H, representative homodecoupled ¹H NMR spectra of PLA, Molecular structure of **4** and **5** and ln([LA]₀/[LA]_t) versus time plot for bulk polymerization of LA.

Acknowledgments

We thank NSERC of Canada, the Canada Foundation for Innovation, the Provincial Government of Newfoundland and Labrador, and Memorial University for Financial Support. JMBs thanks Women in Science and Engineering High-School Summer Student Employment Program. NI thanks Dr. Pawel Horeglad (University of Warsaw) for advice on tacticity calculations.

[§] As with all processes under high pressure, appropriate safety precautions must be taken

Table 5. Summary of crystal data for compounds **L2H**, **1-5**

Compounds	L2H	1	2	3	5
Formula	C ₂₀ H ₃₄ N ₂ O	C ₄₇ H ₇₄ N ₄ O ₂ Zn	C ₃₈ H ₆₄ N ₄ O ₂ Zn ₂	C ₅₈ H ₉₂ N ₄ O ₂ Zn ₂	C ₇₉ H ₁₁₂ N ₄ O ₄ Zn ₂
Formula Weight	318.50	792.51	739.71	1008.15	1312.54
Crystal System	Triclinic	Monoclinic	Triclinic	Triclinic	Monoclinic
Space Group	P-1	C2/c	P-1	P-1	P2/c
a/ Å	6.1799(14)	10.0658(11)	9.6308(9)	9.206(14)	24.314(4)
b/ Å	8.4415(18)	17.945(2)	11.0488(11)	11.540(19)	10.9529(17)
c/ Å	10.081(2)	25.003(3)	19.6721(19)	13.902(20)	28.023(4)
α/ °	67.242(7)	90	100.023(5)	92.493(13)	90
β/ °	78.354(11)	99.377(3)	97.146(5)	93.888(18)	94.232(4)
γ/ °	89.180(12)	90	108.791(4)	111.02(3)	90
V/ Å ³	473.76(17)	4455.8(9)	1914.6(3)	1372(4)	7442.7(20)
T/K	153	153	153	153	153
Z	1	4	2	1	4
D _c / g/cm ³	1.116	1.181	1.283	1.220	1.171
F(000)	176	1720	792	544	2824
μ(MoKα)/ cm ⁻¹	0.68	5.92	12.89	9.18	6.94
Total reflections	3883	28248	20078	14165	96494
Unique reflections	1914 ($R_{\text{int}} = 0.0167$)	4605 ($R_{\text{int}} = 0.0216$)	20078 ($R_{\text{int}} = 0.000$)	5600 ($R_{\text{int}} = 0.0314$)	15414 ($R_{\text{int}} = 0.0563$)
No. of observations	1904	4605	20078	5600	15414
Reflections $I > 2\sigma I$	209	4503	18150	5239	14312
$R(I > 2\sigma I)$	0.0348	0.0338	0.0905	0.0540	0.0643
wR2 (all reflections)	0.0961	0.0924	0.2538	0.1280	0.1574
GOF	1.049	1.038	1.144	1.120	1.172

Table 6. Summary of crystal data for compounds **6-7**

Compounds	6	7
Formula	C ₄₄ H ₇₆ N ₄ O ₄ Zn ₂	C ₅₆ H ₈₆ N ₂ O ₄ Zn ₂
Formula Weight	855.87	982.07
Crystal System	Triclinic	Triclinic
Space Group	P-1	P-1
a/ Å	8.960(3)	10.9384(15)
b/ Å	9.099(3)	11.4289(15)
c/ Å	14.779(6)	11.9898(16)
α/ °	81.33(3)	102.923(8)
β/ °	76.04(2)	106.541(7)
γ/ °	76.04(2)	107.637(8)
V/ Å ³	1123.8(7)	1288.1(3)
T/K	153	153
Z	1	1
D _c / g/cm ³	1.265	1.266
F(000)	460	528
μ(MoKα)/ cm ⁻¹	11.11	9.77
Total reflections	8979	15846
Unique reflections	4141 ($R_{\text{int}} = 0.0939$)	15846 ($R_{\text{int}} = 0.000$)
Reflections $I > 2\sigma I$	2984	14915
No. of parameters	245	290
$R(I > 2\sigma I)$	0.1060	0.1061
wR2 (all reflections)	0.2132	0.2854
GOF	1.149	1.248

- [1] D. J. Doyle, V. C. Gibson, A. J. P. White, *Dalton Trans.* **2007**, 358.
[2] C.-A. Huang, C.-L. Ho, C.-T. Chen, *Dalton Trans.* **2008**, 3502.
[3] C.-A. Huang, C.-T. Chen, *Dalton Trans.* **2007**, 5561.
[4] J. Ejfeler, K. Krauzy-Dziedzic, S. Szafert, L. B. Jerzykiewicz, P. Sobota, *Eur. J. Inorg. Chem.* **2010**, 3602.
[5] X. Zhang, T. J. Emge, K. C. Hultzsch, *Organometallics* **2010**, 29, 5871.
[6] A. D. Schofield, M. L. Barros, M. G. Cushion, A. D. Schwarz, P. Mountford, *Dalton Trans.* **2009**, 85.
[7] W.-C. Hung, C.-C. Lin, *Inorg. Chem.* **2009**, 48, 728.
[8] L. E. Breyfogle, C. K. Williams, J. V. G. Young, M. A. Hillmyer, W. B.

Tolman, *Dalton Trans.* **2006**, 928.

- [9] E. L. Marshall, V. C. Gibson, H. S. Rzepa, *J. Am. Chem. Soc.* **2005**, 127, 6048.
[10] Y. Sarazin, V. Poirier, T. Roisnel, J.-F. Carpentier, *Eur. J. Inorg. Chem.* **2010**, 3423.
[11] D. J. Dahrenbourg, W. Choi, O. Karroonirun, N. Bhuvanesh, *Macromolecules* **2008**, 41, 3493.
[12] H. E. Dyer, S. Huijser, A. D. Schwarz, C. Wang, R. Duchateau, P. Mountford, *Dalton Trans.* **2008**, 32.
[13] A. Amgoune, C. M. Thomas, J.-F. Carpentier, *Macromol. Rapid Commun.* **2007**, 28, 693.
[14] G. Labourdette, D. J. Lee, B. O. Patrick, M. B. Ezhova, P. Mehrkhodavandi, *Organometallics* **2009**, 28, 1309.
[15] L. Wang, H. Ma, *Dalton Trans.* **2010**, 39, 7897.
[16] C. K. Williams, L. E. Breyfogle, S. K. Choi, W. Nam, V. G. Young, M. A. Hillmyer, W. B. Tolman, *J. Am. Chem. Soc.* **2003**, 125, 11350.
[17] M. H. Chisholm, J. C. Gallucci, H. Zhen, J. C. Huffman, *Inorg. Chem.* **2001**, 40, 5051.
[18] M. H. Chisholm, Z. Zhou, *J. Mater. Chem.* **2004**, 14, 3081.
[19] C. K. Williams, N. R. Brooks, M. A. Hillmyer, W. B. Tolman, *Chem. Commun.* **2002**, 2132.
[20] J. LewiÅski, P. Horeglad, M. Dranka, I. Justyniak, *Inorg. Chem.* **2004**, 43, 5789.
[21] S. Groysman, E. Sergeeva, I. Goldberg, M. Kol, *Inorg. Chem.* **2005**, 44, 8188.
[22] S. Gendler, S. Segal, I. Goldberg, Z. Goldschmidt, M. Kol, *Inorg. Chem.* **2006**, 45, 4783.
[23] L. M. Broomfield, Y. Sarazin, J. A. Wright, D. L. Hughes, W. Clegg, R. W. Harrington, M. Bochmann, *J. Organomet. Chem.* **2007**, 692, 4603.
[24] J.-T. Issenhuth, J. Pluvinage, R. Welter, S. Bellemain-Laponnaz, S. Dagorne, *Eur. J. Inorg. Chem.* **2009**, 4701.
[25] V. Poirier, T. Roisnel, J.-F. Carpentier, Y. Sarazin, *Dalton Trans.* **2011**, 40, 523.
[26] J. D. Farwell, P. B. Hitchcock, M. F. Lappert, G. A. Luinstra, A. V. Protchenko, X.-H. Wei, *J. Organomet. Chem.* **2008**, 693, 1861.
[27] L. Nikolic, I. Ristic, B. Adnadjevic, V. Nikolic, J. Jovanovic, M. Stankovic, *Sensors* **2010**, 10, 5063.
[28] S. Jing, W. Peng, Z. Tong, Z. Baoxiu, *J. Appl. Polym. Sci.* **2006**, 100, 2244.
[29] M. R. Kember, A. Buchard, C. K. Williams, *Chem. Commun.* **2011**, 47, 141.
[30] M. North, R. Pasquale, C. Young, *Green Chem.* **2010**, 12, 1514.
[31] K. L. Collins, L. J. Corbett, S. M. Butt, G. Madhurambal, F. M. Kerton, *Green Chem. Lett. Rev.* **2007**, 1, 31

- [32] F. M. Kerton, S. Holloway, A. Power, R. G. Soper, K. Sheridan, J. M. Lynam, A. C. Whitwood, C. E. Willans, *Can. J. Chem.* **2008**, *86*, 435.
- [33] J. Ejfler, S. Szafert, K. Mierzwicki, L. B. Jerzykiewicz, P. Sobota, *Dalton Trans.* **2008**, 6556.
- [34] A. Gao, Y. Mu, J. Zhang, W. Yao, *Eur J. Inorg. Chem.* **2009**, 3613.
- [35] K. Nakano, K. Nozaki, T. Hiyama, *J. Am. Chem. Soc.* **2003**, *125*, 5501.
- [36] I. J. Bruno, J. C. Cole, M. Kessler, J. Luo, W. D. S. Momerwell, L. H. Purkis, B. R. Smith, R. Taylor, R. I. Cooper, S. E. Harris, A. G. Orpen, *J. Chem. Inf. Comput. Sci.* **2004**, *44*, 2133.
- [37] J. Hunger, S. Blaurock, J. Sieler, *Anorg. Allg. Chem.* **2005**, *631*, 472.
- [38] M. R. P. Van Vliet, J. T. B. H. Jastrzebski, G. Van Koten, K. Vrieze, A. L. Spek, *J. Organomet. Chem.* **1983**, *251*, c17.
- [39] H.-Y. Chen, H.-Y. Tang, C.-C. Lin, *Macromolecules* **2006**, *39*, 3745.
- [40] A. Banerjee, S. Ganguly, T. Chattopadhyay, K. Sabnam Banu, A. Patra, S. Bhattacharya, E. Zangrando, D. Das, *Inorg. Chem.* **2009**, *48*, 8695.
- [41] K. Nakano, T. Hiyama, K. Nozaki, *Chem. Commun.* **2005**, 1871.
- [42] Y. Sarazin, J. A. Wright, D. A. J. Harding, E. Martin, T. J. Woodman, D. L. Hughes, M. Bochmann, *J. Organomet. Chem.* **2008**, *693*, 1494.
- [43] A. R. F. Cox, V. C. Gibson, E. L. Marshall, A. J. P. White, D. Yeldon, *Dalton Trans.* **2006**, 5014.
- [44] C. M. Silvernail, L. J. Yao, L. M. R. Hill, M. A. Hillmyer, W. B. Tolman, *Inorg. Chem.* **2007**, *46*, 6565.
- [45] F. Qian, K. Liu, H. Ma, *Dalton Trans.* **2010**, *39*, 8071.
- [46] L. F. Sanchez-Barba, C. Alonso-Moreno, A. Garces, M. Fajardo, J. Fernandez-Baeza, A. Otero, A. Lara-Sánchez, A. M. Rodriguez, I. Lopez-Solera, *Dalton Trans.* **2009**, 8054.
- [47] A. Garcés, L. F. Sánchez-Barba, C. Alonso-Moreno, M. Fajardo, J. Fernández-Baeza, A. Otero, A. Lara-Sánchez, I. López-Solera, A. M. Rodríguez, *Inorg. Chem.* **2010**, *49*, 2859.
- [48] C. Zhang, Z.-X. Wang, *Appl. Organomet. Chem.* **2009**, *23*, 9.
- [49] H. Zhu, E. Y. X. Chen, *Organometallics* **2007**, *26*, 5395.
- [50] F. Drouin, P. O. Oguadinma, T. J. J. Whitehorne, R. E. Prud'homme, F. Schaper *Organometallics* **2010**, *29*, 2139.
- [51] B. M. Chamberlain, M. Cheng, D. R. Moore, T. M. Ovitt, E. B. Lobkovsky, G. W. Coates, *J. Am. Chem. Soc.* **2001**, *123*, 3229.
- [52] T. Sakakura, K. Kohno, *Chem. Commun.* **2009**, 1312.
- [53] D. J. Daresbourg, S. J. Lewis, J. L. Rodgers, J. C. Yarbrough, *Inorg. Chem.* **2003**, *42*, 581.
- [54] Y.-M. Shen, W.-L. Duan, M. Shi, *J. Org. Chem.* **2003**, *68*, 1559.
- [55] F. Li, L. Xiao, C. Xia, B. Hu, *Tetrahedron Lett.* **2004**, *45*, 8307.
- [56] V. Caló, A. Nacci, A. Monopoli, A. Fanizzi, *Org. Lett.* **2002**, *4*, 2561.
- [57] J. Sun, J. Ren, S. Zhang, W. Cheng, *Tetrahedron Lett.* **2009**, *50*, 423.
- [58] D. J. Daresbourg, J. L. Rodgers, R. M. Mackiewicz, A. L. Phelps, *Catal. Today* **2004**, *98*, 485.
- [59] N. Ikpo, S. M. Butt, K. L. Collins, F. M. Kerton, *Organometallics* **2009**, *28*, 837.
- [60] M. D. Eelman, J. M. Blacquiere, M. M. Moriarty, D. E. Fogg, *Angew. Chem. Int. Ed.* **2008**, *47*, 303.
- [61] a) CrystalClear: Rigaku Corporation, 1999. CrystalClear Software User's Guide, Molecular Structure Corporation, © 2000, Pflugrath, J. W. *Acta Cryst.*, **1999**, *D55*, 1718-1725; b) SHELX97: Sheldrick, G. M. *Acta Cryst.* **2008**, *A64*, 112; c) SIR92: Altomare, A.; Cascarano, G.; Giacovazzo, C.; Guagliardi, A.; Burla, M.; Polidori, G.; Camalli, M. J. *J. Appl. Cryst.*, **1994**, *27*, 435; d) DIRDIF99: Beurskens, P. T.; Admiraal, G.; Beurskens, G.; Bosman, W. P.; de Gelder, R.; Israel, R.; Smits, J. M. M. The DIRDIF-9 9 program system, Technical Report of the Crystallography Laboratory, University of Nijmegen, The Netherlands, 1999; e) Cromer, D. T.; Waber, J. T. *International Tables for X-ray Crystallography*, Vol. IV, The Kynoch Press, Birmingham, England, Table 2.2 A, **1974**; f) Ibers, J. A.; Hamilton, W. C. *Acta Crystallogr.*, **1964**, *17*, 781; g) Creagh, D. C.; McAuley, W. J. *International Tables for Crystallography*, Vol C, (Wilson, A. J. C. ed.), Kluwer Academic Publishers, Boston, **1992**, Table 4.2.6.8, pp. 219-222; h) Creagh, D. C.; Hubbell, J. H. *International Tables for Crystallography*, Vol C, (Wilson, A. J. C. ed.), Kluwer Academic Publishers, Boston, **1992**, Table 4.2.4.3, pp. 200-206; i) CrystalStructure 3.7.0: Crystal Structure Analysis Package, Rigaku and Rigaku/MSC, 9009 New Trails Dr. The Woodlands TX 77381 USA, 2000-2005; j) Watkin, D. J.; Prout, C. K.; Carruthers, J. R.; Betteridge, P. W. CRYSTALS Issue 10, Chemical Crystallography Laboratory, Oxford, UK, 1996; k) Spek, A.L. *J. Appl. Cryst.* **2003**, *36*, 7-13.

Received: ((will be filled in by the editorial staff))
 Published online: ((will be filled in by the editorial staff))

Entry for the Table of Contents

Layout 1:

New Zn^{II} complexes have been prepared and structurally characterized including a rare example of a dimetallic Zn species containing cis-alkyl groups. Their reactivity in both solution and bulk polymerization of *rac*-lactide and ϵ -caprolactone is presented, including reactions under microwave conditions. Interestingly, their behaviour is different to morpholiny analogues.



Zinc Complexes of Piperazinyl-aminephenolate Ligands: Synthesis, Characterization and Ring-Opening Polymerization Activity

Nduka Ikpo,^[a] Lisa N. Saunders,^[a] Jillian L. Walsh,^[a] Jennifer M. B. Smith,^[a] Louise N. Dawe,^[b] and Francesca M. Kerton *^[a] Page No. – Page No.

Keywords: Zinc /Alkyl / Alkoxide / Phenoxide / Ring-opening polymerization/ Lactide

Supporting Information

Zinc Complexes of Piperazinyl-aminephenolate Ligands: Synthesis, Characterization and Ring-Opening Polymerization Activity

*Nduka Ikpo, Lisa N. Saunders, Jillian L. Walsh, Jennifer M. B. Smith, Louise N. Dawe, and Francesca M. Kerton**

Department of Chemistry, Memorial University of Newfoundland, St. John's, Newfoundland, Canada A1B 3X7

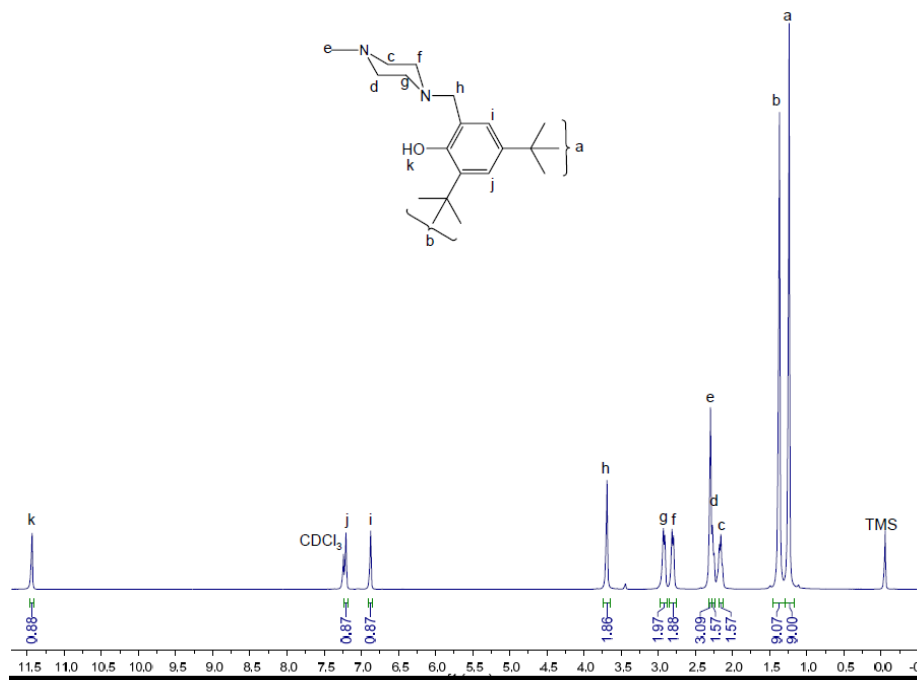


Fig. S1 ^1H NMR spectrum of **L2H** (CDCl_3 , 500 MHz, 288 K).

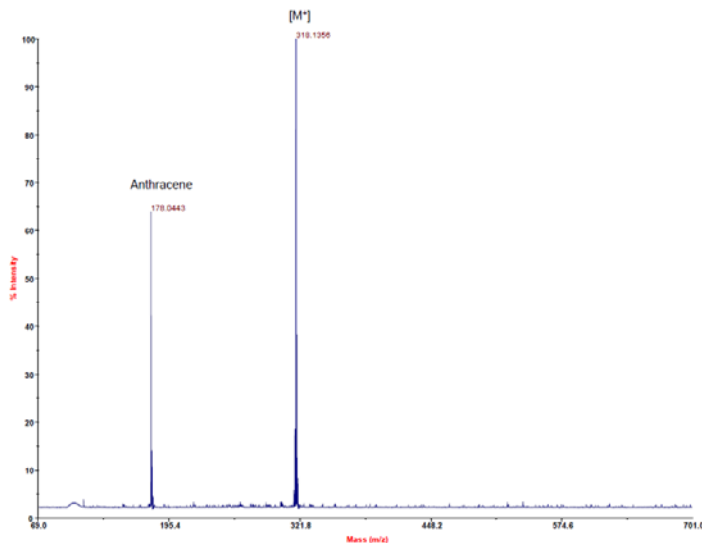


Fig. S2 Mass spectrum of **L2H** (MALDI, matrix: anthracene)

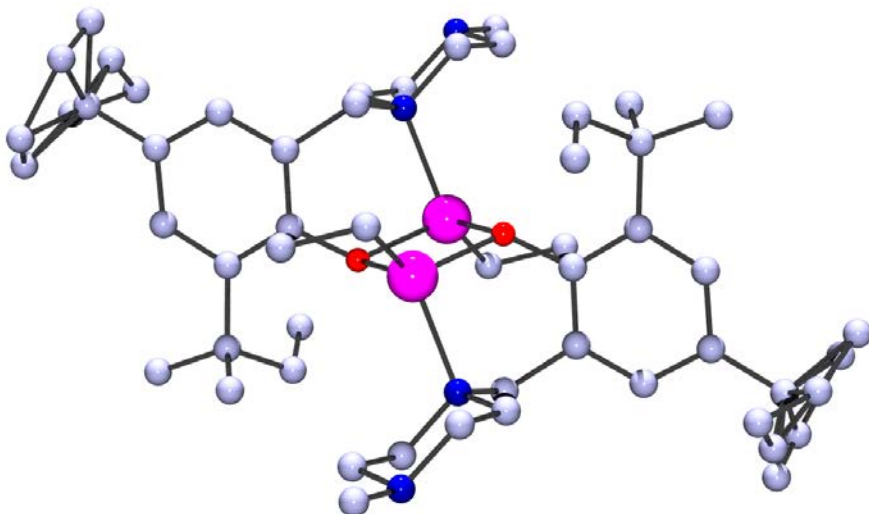


Fig. S3 Molecular structure of **4**. (Weak diffraction and twinning yielded a data set containing severely disordered *para-t*-amyl group)

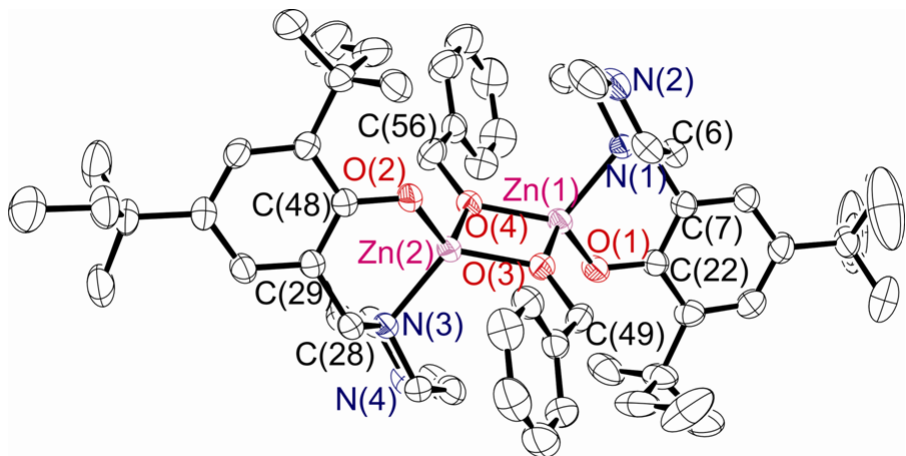


Fig. S4 Molecular structure of **5**. (50% thermal ellipsoids; H atoms excluded for clarity). Selected bond lengths (\AA) and bond angles ($^{\circ}$): Zn(1)-O(1), 1.901(2); Zn(1)-O(4), 1.953(2); Zn(1)-O(3), 1.974(2); Zn(1)-N(2), 2.061(2); Zn(1)-Zn(2), 2.9459(5); Zn(2)-O(2), 1.900(2); Zn(2)-O(3), 1.954(2); Zn(2)-O(4), 1.970(2); Zn(2)-N(4), 2.059(2); O(1)-C(22), 1.342(3); O(2)-C(48), 1.346(4); O(3)-C(49), 1.411(3); O(4)-C(56), 1.414(3); N(1)-C(4), 1.454(4); N(1)-C(2), 1.459(4); O(1)-Zn(1)-O(4), 121.09(9); O(1)-Zn(1)-O(3), 115.98(9); O(4)-Zn(1)-O(3), 82.71(8); O(1)-Zn(1)-N(2), 101.29(9); O(4)-Zn(1)-N(2), 119.11(9); O(3)-Zn(1)-N(2), 117.34(9); O(1)-Zn(1)-Zn(2), 129.55(6); O(4)-Zn(1)-Zn(2), 41.56(6); O(3)-Zn(1)-Zn(2), 41.15(6); N(2)-Zn(1)-Zn(2), 128.95(7); O(2)-Zn(2)-O(3), 121.70(9); O(2)-Zn(2)-O(4), 116.84.

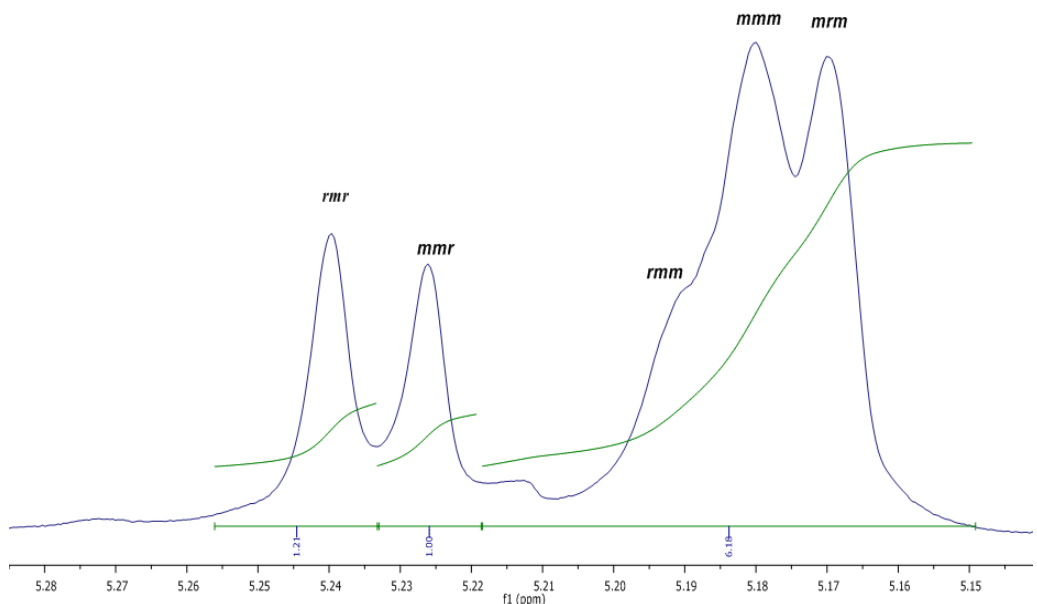


Fig. S5 Homonuclear decoupled ^1H NMR spectrum of the methane region of PLA prepared with **6**/rac-lactide (bulk polymerization) at 130 °C for 30 min (500 MHz, CDCl_3)

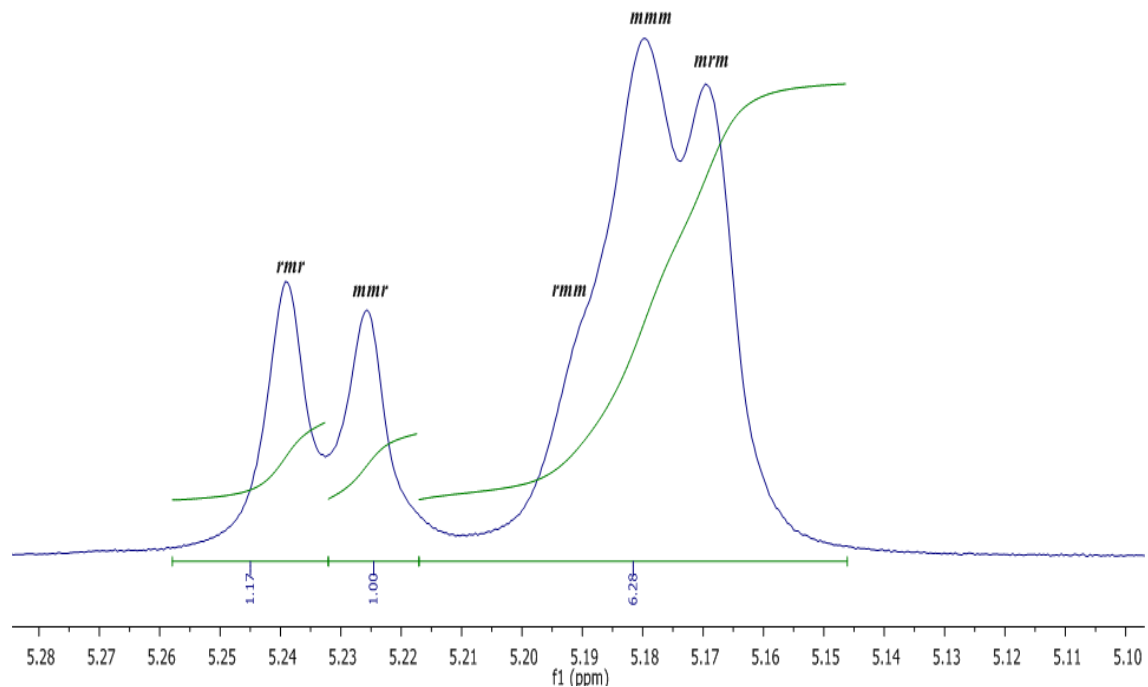


Fig. S6 Homonuclear decoupled ^1H NMR spectrum of the methane region of PLA prepared with **3**/ BuOH /rac-lactide (solution polymerization) at 130 °C for 30 min (500 MHz, CDCl_3)

Bulk Ring-Opening Polymerization of *rac*-Lactide by **5** and **6** at 130 °C

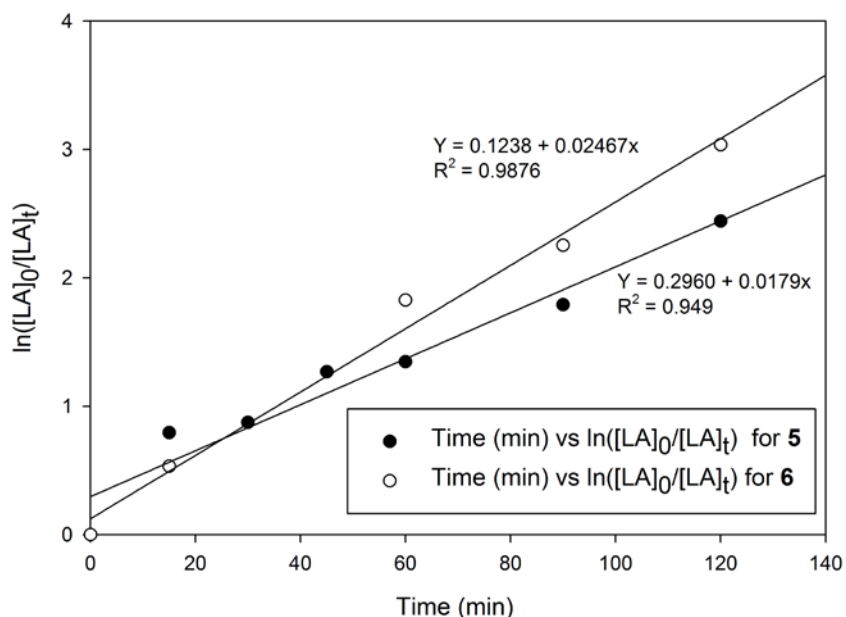


Fig. S7 Plots of $\ln([LA]_0/[LA]_t)$ versus time for the bulk polymerization of *rac*-lactide initiated by **5** and **6**: [LA]/[Zn] = 100 at 130 °C. **5** (filled circles) and **6** (hollow circles).